

FINAL TECHNICAL MEMORANDUM

# Physical Modeling Experiments to Guide River Restoration Projects:

## Channel-floodplain Redesign Experiments

*Prepared for*

CALFED Ecosystem Restoration Program  
(Contract No. ERP-02D-P55)

*Prepared by*

Stillwater Sciences  
Berkeley, California

Department of Earth and Planetary Science  
University of California, Berkeley, California

and

Department of Geosciences  
San Francisco State University, San Francisco, California

July 2007





Table of Contents

**1 INTRODUCTION ..... 1**  
1.1 Impetus for Channel-floodplain Redesign Experiments and Experimental Questions..... 2

**2 OVERVIEW OF THE CHANNEL-FLOODPLAIN REDESIGN EXPERIMENTS AND ANALYSIS ..... 2**  
2.1 Preliminary Experiments ..... 3  
2.2 The Effects of Variable Discharge on Channel Morphology..... 3  
    2.2.1 Conditions Necessary to Create Meandering Channels..... 4

**3 SUMMARY OF MAJOR FINDINGS RELATED TO CHANNEL-FLOODPLAIN REDESIGN AND IMPLICATIONS FOR CHANNEL-FLOODPLAIN REDESIGN..... 5**

**4 REFERENCES..... 5**

**APPENDICES**

**Appendix A** The influence of variable discharge on the morphodynamics of a laterally migrating model meandering river



# 1 INTRODUCTION

California Bay-Delta agencies have identified a number of strategies for restoring Bay-Delta tributaries. Three such strategies include: 1) injecting gravel to compensate for the loss of coarse sediment trapped behind dams and mined from the channel; 2) removing diversion dams to open access to upstream habitats and restore fluvial geomorphic continuity; and 3) reconstructing river channels and floodplains to be more in balance with a regulated flow regime as a means of restoring fluvial geomorphic processes. Funding has been provided for several projects that employ these restoration strategies on the Tuolumne, Merced, and Stanislaus Rivers, and Clear Creek. Experience with these projects highlights several significant gaps in the scientific understanding of fluvial geomorphic processes, particularly concerning how river bed texture and mobility are influenced by episodic sediment delivery, and how floodplain and channel geometry and stability are influenced by changes in the discharge and sediment supply regimes. The lack of a strong scientific basis for design decisions has often forced project implementers to rely on their professional judgment, which is typically based on qualitative conceptual models and site-specific past experience.

To further the quantitative understanding behind restoring rivers, Stillwater Sciences, in conjunction with the University of California Berkeley and San Francisco State University, was awarded a project entitled 'Physical Modeling to Guide River Projects' (CALFED Ecosystem Restoration Program Contract No. ERP-02D-P55). The purpose of the project was to build two state-of-the-art flumes and conduct a series of physical modeling experiments to address some of the fundamental and unresolved scientific questions underlying the river restoration strategies of gravel augmentation, dam removal, and floodplain-channel redesign. The experiments were conducted at the University of California Richmond Field Station and focused on achieving two broad goals. First, the experiments focused on developing a mechanistic understanding of river channel response to episodic delivery of bedload-sized sediments, as occurs in both gravel augmentation and dam removal projects. Second, the experiments focused on establishing quantitative relationships between channel morphologic dynamics and evolution, flow discharge, and sediment supply. As these overarching research goals deal with areas of inquiry in which limited progress has been made in previous field, experimental, and theoretical studies, the results from this project from both physical and numerical modeling represent significant contributions towards furthering the state-of-the-science for designing, implementing, and monitoring river restoration projects for California watersheds and beyond.

This technical memorandum describes the key points from the channel-floodplain redesign experiments. Two other memoranda that describe the key points from the gravel augmentation and dam removal experiments are also being submitted concurrently. The purpose of this memorandum is to provide a brief discussion of the experimental questions, the experimental design, and summarizes the results, analysis, and key findings/implications for the physical modeling associated with channel-floodplain redesign. Although experiments have been completed under the current CALFED ERP contract, the channel-floodplain redesign experimental program is ongoing. Detailed discussions of the entire channel-floodplain redesign experimental program can be found in several manuscripts that are either in preparation or have been submitted to professional scientific journals. Attached to this memorandum is a copy of a completed manuscript currently in preparation for potential publication in a scientific journal that details one set of comprehensive channel-floodplain redesign experiments ('The influence of variable discharge on the morphodynamics of a laterally migrating model meandering river,' see Appendix A).

## 1.1 Impetus for Channel-floodplain Redesign Experiments and Experimental Questions

Downstream of large dams, channel dimensions are typically scaled to the pre-dam hydrograph regime, but under the current hydrograph regime sediment transport and floodplain inundation occur less frequently than under natural conditions (typically every 1.5 years). Throughout the Central Valley and elsewhere, channels are being rebuilt to accommodate the current flow regime and increase sediment transport and floodplain inundation. These channels are often constructed as gravel-bed, meandering rivers because of their high habitat diversity and ability to support spawning salmonids. Three primary questions related to these types of projects include:

1. How do channels respond to variable flow,
2. What conditions are necessary to promote meandering, and
3. What are the effects of sediment supply on channel morphology?

We have conducted experiments to address the first two questions listed above. The third question will be addressed by experiments that will begin in Fall, 2007. Results from these experiments represent a significant step toward guiding future channel-floodplain reconstruction projects and can also be used to guide the minimum time required to assess the success or failure of a project.

## 2 OVERVIEW OF THE CHANNEL-FLOODPLAIN REDESIGN EXPERIMENTS AND ANALYSIS

The greatest challenge of this research was creating a self-formed, single-thread channel in a laboratory flume. Researchers have been trying to create self-formed channels in laboratory flumes for over 60 years (*e.g.*, Friedkin, 1945; Wolman and Brush, 1957; Schumm and Kahn, 1972; Eaton and Church, 2004). The first successful attempt was by Smith (1998), who created small (< 4 cm wide), steep (slope = 0.015) meandering channels in a laboratory using cohesive materials such as diatomaceous earth and kaolinite clay. The experiments by Smith indicate that increasing bank strength promotes meander development in laboratory flumes. For our experiments, we sought to create meandering channels with granular beds (*i.e.*, non-cohesive substrate) in an effort to replicate processes in gravel-bed channels.

In the experiments discussed below, we used alfalfa sprouts to provide bank strength. Gran and Paola (2001) used alfalfa in their laboratory experiments in order to reduce the channel braiding index and Tal and Paola (2007) used alfalfa in their laboratory experiments to transform braided channels into single-threaded channels. The one drawback to using alfalfa sprouts is that they need to be replanted relatively frequently (every 8–16 hours) and allowed to grow for 7–10 days, depending on weather. These factors slow down experiments considerably, but attempts to use material other than alfalfa sprouts (*e.g.*, granular sediment only, mildly cohesive sediments, artificial vegetation) were not successful.

We conducted the experiments in two basins. The first basin is 6.1 m long and 3.7 m wide (*i.e.*, the small basin). This basin has an adjustable slope and recirculates water but not sediment. The second basin is 16 m long and 6.1 m wide (*i.e.*, the large basin). This basin has a fixed slope and also recirculates water. Rather than scaling a particular channel, we chose to model a channel representative of typical natural channels using the methods outlined by Parker *et al.* (2003).

## 2.1 Preliminary Experiments

We conducted several preliminary experiments in an attempt to create a meandering channel. These experiments were conducted in the small basin with a channel slope of 0.01, and alfalfa sprouts were used to provide bank strength. Coarse and fine sediment were fed separately, with the coarse sediment transported as bedload and the fine sediment transported as suspended load. The floodplain was made up of the same sediment as the coarse feed, which was sand with a median grain size of 0.95 mm. The fine sediment feed consisted of ground silica with a median diameter of 0.027 mm. We used two initial channel configurations for the experiments: a sine wave with two bends, and an initial bend followed by a straight section. In both experiments, the results were similar, indicating that the initial channel configuration did not significantly affect the results. In these experiments the channel developed bars, but the channel aggraded upstream of the first bend and caused headcuts to propagate up the flume. These headcuts caused chute cutoffs, and the channel eventually straightened due to neck cutoffs. The headcuts created an unstable condition and the channel width continually increased.

These preliminary experiments were encouraging because we were able to build bars and create cutoffs and oxbow lakes; however, the channels were not stable through time. The results of these experiments are similar to those observed in recently published experiments by Peakall *et al.* (2007) who used ground silica to provide bank strength in meandering channels. We believed that this channel instability occurred for three reasons. The first reason was that our Froude numbers were too high (averaging approximately 0.8), and hydraulic jumps formed at the front of bars. Meandering channels with such high Froude numbers are rare (Parker, 1976) and the high Froude numbers may have promoted chute cutoffs. The second problem was that although the ground silica primarily traveled in suspension, particles that did settle onto the bed were very difficult to re-entrain and their presence on the bed promoted headcut propagation. Finally, we determined that the small basin was too small to accommodate more than one bend, which led us to construct the large basin (described below).

## 2.2 The Effects of Variable Discharge on Channel Morphology

While we were constructing the large basin, we conducted additional experimental runs in the small basin. For these runs, we reduced the slope of the small basin to 0.005 to test the effects of variable discharge on the channel morphology (see Attachment for a full description of these experiments, results, and analysis). Because of the lower slope, we set the new initial channel to a width of 50 cm and set the planform channel geometry to one low-amplitude bend. We hypothesized that a full range of flows, characteristic of pre-dam conditions in natural streams, are critical to attach bars to floodplains and to maintain a meandering morphology. Similar to the preliminary experiments, bank strength was provided using alfalfa sprouts, but we also added a thin layer of uniformly applied ground silica on top of the coarse floodplain sediments. We used an asymmetrical, stepped hydrograph that ranged from the critical discharge for initiation of sediment transport up to a discharge equal to twice the bankfull flow. We also co-varied the bedload feed rate with the discharge. We did not feed any suspended sediment during the experiments presented here based on problems created by their use during our preliminary runs.

From these experiments, we discovered that the overbank flows increased lateral migration rates, bar-connection with the floodplain, and aided in maintaining a relatively stable channel width. Accumulation of sediment within the channel occurred during the rising limb and peak, but a balance of total sediment input and output was eventually reached during the relatively longer falling limb steps, where output rates were greater. We additionally discovered that the ratio of deposition to erosion rates at three channel cross-sections were not a function of discharge, but were dependent on the channel position relative to the apex of the migrating bend where lateral migration rates were greatest. In addition, higher rates of change at the cross-sections generally occurred during the rising limb as opposed to the falling limb.

## 2.2.1 Conditions Necessary to Create Meandering Channels

The final experiments were conducted in the large 6.1 m by 16 m basin and were designed to investigate the conditions necessary to create meandering channels. The size of this basin allowed us to overcome many of the shortcomings of the small basin, including accommodating a channel with more than one bend and minimizing the effects of the inflow and outflow boundary conditions. The large basin has a set slope of 0.004 and the initial channel was 0.4-m wide and 0.019-m deep. Similar to the experiments in the small basin, we used alfalfa sprouts to generate bank strength. We hypothesized that meandering channels require: (1) additional bank strength from vegetation or cohesive materials; (2) overbank flows as observed in the experiments described above; and (3) fine sediment to deposit in the trough (chute) between the floodplain and the point bar. We used a lightweight plastic as our model fine sediment to avoid scaling difficulties associated with using fine sediment. We have completed experiments with a simple two-stage hydrograph and are currently conducting experiments with a constant bankfull hydrograph to test whether overbank flows are a necessary condition for meandering rivers. For these experiments, the coarse sediment had a median diameter of 0.85 mm, while the fine (plastic) sediment had a median size of 0.35 mm, with a specific gravity of 1.3–1.5. The low-density sediment helps to minimize scaling difficulties associated with the use of silt and clay. Our flood hydrographs were a simple two-stage hydrograph consisting of bankfull flow (1.8 l/s) and an overbank flow (2.7 l/s). The bankfull flow was run for 5.5 hours for every 1.5 hours of the overbank flow.

The experiments with the two-stage hydrograph were run for over 70 hours without the channel braiding, and the width of the almost entirely self-formed channel stabilized. Cross section surveys showed that bar growth paces with bank erosion and bar tops grew to just below the elevation of the floodplain. Bars were constructed from sediment derived from erosion of the upstream bank rather than sediment fed from upstream. Bars were connected to the floodplain at their upstream end but not at their downstream end. Although chutes remained behind the downstream end of the bars, they did not expand. The sinuosity, bend amplitude, and bend wavelength of the channel increased through time until a chute cutoff occurred. Following the chute cutoff, the channel maintained a single-thread pattern. Overall, the self-formed channels we have created in the laboratory are stable over long periods, replicate conditions observed in the field, and are sufficient to test our hypotheses on the effects of sediment supply on bar morphology. These experiments have produced the first successful, meandering channel created in a laboratory, and we can now isolate variables (*e.g.*, discharge, sediment supply) to test their effect on meander morphology.

The second part of this experiment (*i.e.*, using a constant bankfull hydrograph) is ongoing, and will continue throughout the summer of 2007. A paper summarizing the second part of the experiments is in preparation and will be submitted to a professional scientific journal at the completion of these experiments. Following these experiments, we will continue our research by examining the role of sediment supply in channel morphology, specifically how changes in sediment supply are accommodated by topographic steering, and the feedbacks between topographic steering and bar growth and morphology. These experiments will be used to develop and test models of flow through bends that account for changes in sediment supply changes from upstream, which can then be applied to channels in a variety of environments.

### 3 SUMMARY OF MAJOR FINDINGS RELATED TO CHANNEL-FLOODPLAIN REDESIGN AND IMPLICATIONS FOR CHANNEL-FLOODPLAIN REDESIGN

- Alfalfa sprouts increase bank strength, and their use can enable physical modeling of self-formed channels provided that the basin is large enough and the Froude numbers are low enough.
- Overbank flows are needed, to deliver sediment into the chute separating the bar and inner bank, and to grow bars vertically up to the floodplain elevation. Ongoing experiments in the large basin will test whether overbank flows are required to attach bars to floodplains.
- Bar morphology differs as a result of overbank flows and bankfull flows.
- Following an overbank flood, the longer time periods of the falling limb at a specific discharge allow for equilibrium between the total sediment input and output.
- Bars were constructed from erosion of the bank immediately upstream and not from sediment flux in, indicating that bank erosion is important for bar formation and maintenance.
- Taken together, our experiments indicate that bank strength exceeding that available with only granular sediment is necessary for meandering to occur. In addition, overbank flows appear to help attach bars to floodplains.

### 4 REFERENCES

- Eaton, B.C., and M. Church. 2004. A graded stream response relation for bed load – dominated streams. *Journal of Geophysical Research* 109: F03011, doi:10.1029/2003JF000062.
- Friedkin, J.F. 1945. A laboratory study of the meandering of alluvial rivers. *U.S. Waterways Experimental Station Report*, U.S. Army Corps of Eng., Vicksburg, MS, 40 pp.
- Gran, K., and C. Paola. 2001. Riparian vegetation controls on braided stream dynamics. *Water Resources Research* 37: 3275–3283.
- Peakall, J., P.J. Ashworth, and J.L. Best. 2007. Meander-bend evolution, alluvial architecture, and the role of cohesion in sinuous river channels: A flume study. *Journal of Sedimentary Research* 77: 197-212.
- Parker G. 1976. On the cause and characteristic scales of meandering and braiding in rivers. *Journal of Fluid Mechanics* 76: 457–480.
- Parker, G., C.M. Toro-Escobar, M. Ramey and S. Beck. 2003. The effect of floodwater extraction on the morphology of mountain streams, *Journal of Hydraulic Engineering* 129: 885–895.
- Schumm, S.A., and H. R. Khan. 1972. Experimental study of channel patterns, *Geological Society of America Bulletin* 83: 1755–1770.
- Smith, C. 1998. Modeling high sinuosity meanders in a small flume. *Geomorphology* 25: 19-30.
- Tal, M. and C. Paola. 2007. Dynamic single-thread channels maintained by the interaction of flow and vegetation. *Geology* 35: 347-350.
- Wolman, M.G. and L. M. Brush. 1961. Factors controlling the size and shape of stream channels in coarse, noncohesive sands. *U.S. Geological Survey Professional Paper*, 282-G. p.183-210.



---

**APPENDIX A**

**The influence of variable discharge on the morphodynamics  
of a laterally migrating model meandering river**

---



**Category: Erosion, Sedimentation, and Geomorphology**

*1825 Geomorphology: fluvial, 1861 Sedimentation, 1862 Sediment transport*

**The influence of variable discharge on the morphodynamics of a laterally migrating model meandering river**

Glen T. Leverich<sup>1,2</sup>, Christian A. Braudrick<sup>3</sup>, Leonard S. Sklar<sup>2</sup>,  
and William E. Dietrich<sup>3</sup>

**Abstract:** Successful restoration of active lateral migration in gravel-bedded, meandering floodplain channels downstream of dams is currently limited by significant uncertainty about the role of variable discharge and sediment supply in driving bank erosion and bar building processes. We conducted a series of experiments to physically model a single-thread, meandering floodplain channel with erodible bed and banks to document bar growth and bank erosion response to a flood hydrograph and determine the conditions necessary for successful floodplain re-design. We hypothesized that overbank flows, characteristic of pre-dam conditions, are critical for developing a dynamic, yet sustainable, stable-width, meandering floodplain river. We explored the role of variable discharge as represented by a stepped flood hydrograph with overbank flows. Significant bar-connection with the floodplain, increased lateral migration rates, and maintenance of a single-thread channel resulted. The highest rates of bank erosion, bar growth, and lateral migration occurred during the overbank flows. We co-varied the bedload feed rate with the discharge so that the sediment flux remained closely balanced over the course of each of the hydrograph runs. Although accumulation occurred during the rising limb and peak steps, equilibrium was eventually reached during the relatively longer falling limb steps, where output rates were greater than input rates signifying the necessity for a longer falling limb than a rising limb to balance the change in sediment storage. At three channel cross-sections, we found that the ratio of deposition rates to erosion rates were not a function of discharge, which was in part due to the controlled rates of sediment input, but rather were dependent on a cross-section's proximity to the apex of the migrating bend (*i.e.*, focus of greatest lateral migration rates). Higher rates of change at the cross-sections generally occurred during the rising limb as opposed to the falling limb for a specific discharge, except if near the bend apex during the falling limb. Our research marks the first attempts at quantifying a model meandering floodplain channel's response to a flood hydrograph and has shown how the components of a hydrograph, specifically overbank flow, influence channel morphology. This work applies directly to influencing restoration design methods that, in the past, have rarely considered the role of higher magnitude flows in shaping the channel and influencing rates of morphologic change.

## INTRODUCTION

Large dams have altered the morphology of many rivers by trapping sediment and by decreasing the recurrence intervals of overbank floods (*Graf, 2005*). The combined effects of reducing flows and eliminating coarse sediment supply causes the channel to incise, the bed to coarsen, and for the channel to be oversized for its typical post-dam discharge (*Williams and Wolman, 1984; Andrews, 1986; Collier et al., 2000*). Vegetation encroachment on the stream margins often occurs due to the reduced flood frequency, resulting in further channel entrenchment and planform homogeneity (*Stillwater Sciences,*

---

<sup>1</sup> Stillwater Sciences, 2855 Telegraph Avenue, Berkeley, CA 94705, USA, email: [glen@stillwatersci.com](mailto:glen@stillwatersci.com), phone: 510-848-8098 ext. 156, fax: 510-848-8398

<sup>2</sup> Department of Geosciences, San Francisco State University, San Francisco, CA 94132, USA, email: [leonard@sfsu.edu](mailto:leonard@sfsu.edu), phone: 415-338-1204

<sup>3</sup> Department of Earth and Planetary Science, University of California, Berkeley, CA 94720, USA, email: [bill@eps.berkeley.edu](mailto:bill@eps.berkeley.edu), phone: 510-642-2633

2001; Tal et al., 2004). In un-dammed rivers peak flows contribute to channel-forming processes, including sediment transport, bank erosion and lateral channel migration. It has been previously suggested that discharge is the “master variable” on stream ecology (Power et al., 1995) and that flow variation is necessary to maintain the ecologic integrity of a stream channel (Doyle et al., 2005). As a result, the morphologic and hydrologic alterations that have been caused by anthropogenic disturbances (i.e., dams) have negatively impacted species such as native salmonid populations that are dependent on the hydrologically dynamic channels for spawning and rearing habitat (Ligon et al., 1995; McBain and Trush, 1997).

In response to the altered physical state of many rivers, river restoration has become accepted as a necessary means to repair channel form and function, and improve ecological habitat (Wohl et al., 2005). However, despite the fact that most restoration projects are followed by little to no monitoring (Palmer et al., 2005), there have been several well-documented cases where reconstructed channels often straighten, widen, braid, or abandon the designed channels (e.g. Williams et al., 1997; Kondolf et al., 2001). These outcomes demonstrate that available tools to guide restoration design were inadequate to account for sediment supply, appropriate selection of channel width, and importantly, the role of higher magnitude flows in shaping the channel and influencing rates of morphologic change in favor of a channel designed to a conceptualized bankfull, or “effective” discharge (Smith and Prestegard, 2005).

Under natural conditions, a meandering river experiences a wide variation of discharges and sediment loads, while laterally migrating across its floodplain and maintaining a relatively stable width (Leopold and Wolman, 1960). This represents an excellent example of a dynamic equilibrium state, whereby constructive and destructive processes, such as bar growth and bank erosion, are in relative balance over time (Andrews, 1982). The principle challenge in restoring any stream is understanding the mechanics involved in maintaining this balance, and creating the necessary conditions in the restoration design. One new restoration technique aims to re-activate sediment transport processes under the post-dam flow regime by building a smaller channel that is sized such that during significant flow events, flow depth is sufficient to transport sediment and inundate the floodplain (e.g., CALFED, 2000; Clear Creek Restoration Team, 2000). However, we lack adequate science-based tools for the selection of an appropriate channel width for a given range of discharge and sediment supply. Because these projects cost millions and are often slow to implement, it is prudent to test new theories on meandering river mechanics and the effects of variable discharge and sediment supply in a controlled laboratory setting.

The purpose of this paper is to report the findings from a series of flume experiments that further the understanding of how to model a single-thread meandering channel and how variable discharge using a stepped flood hydrograph drives channel processes, specifically bar growth and bank erosion. This marks the first time a hydrograph has been incorporated in a physical model of meandering floodplain channel. Previous flume studies have sought to simplify discharge conditions by utilizing either a constant bankfull (i.e., effective discharge) (Schumm and Khan, 1972; Eaton and Church, 2004; Peakall et al., 2007), or a simple low to high stage change (Friedkin, 1945; Smith, 1998). Physical modeling experiments using non-cohesive sediments with minimal flow variance have produced short-lived, low-sinuosity channels with submerged bars that ultimately developed a wide, multi-thread channel (Friedkin, 1945; Ackers and Charlton, 1970; Eaton and Church, 2004). In those experiments, submerged bars never accreted vertically to the floodplain elevation, or bankfull water surface elevation, and remained separated from the inner bank by a narrow chute. Only the thalweg meandered during these experiments as the inner bank either did not advance at all or significantly lagged behind the outer bank migration. Models using cohesive materials have had more success as the resistant banks slowed outer bank migration rates and emergent point bars formed (Schumm and Khan, 1972; Jin and Schumm, 1986; Peakall et al., 2007). However, the bars never accreted to the floodplain elevation and only emerged once the thalweg deepened and the cross-sectional area increased. Erosion eventually ceased in these experiments due to either ossification from clay coating the channel boundary or by the development of a single channel

bend. *Peakall et al.* (2007) recognized that long-term meandering requires bar accretion to the floodplain elevation, which did not occur in their experiments under the imposed constant discharge.

Recently, the effects of hydrographs on channel morphology have been studied in one-dimensional flume experiments (*i.e.*, straight flumes without a floodplain) that demonstrate how channel parameters, such as sediment transport rates, velocity, and flow depth (*Graf and Qu*, 2003), and processes, such as armoring and vertical sorting (*Parker et al.*, 2003; *Hassan et al.*, 2006; *Wong and Parker*, 2006a), track the hydrograph. For example, *Hassan et al.* (2006) found that their constant discharge experiments resulted in bed armoring while short asymmetrical hydrograph (*i.e.*, flashy) experiments resulted in minimal vertical sorting and minor change in the bed surface composition. In a fixed channel bend experiment, *Yen and Lee* (1995) found that the depth of scouring at the outer bank, height of deposition on the bar, and transverse sorting all increased with the degree of unsteady flow (*i.e.*, higher peak and shorter duration). Taken together, these findings suggest that the magnitude, duration, and shape of a hydrograph influence channel morphology and therefore variable flow, not just a single “effective discharge” such as bankfull, should be considered as a key control on river morphology.

The goal of our experiment was to physically model a scaled-down, single-thread meandering floodplain channel in a series of controlled experiments and to examine how bar growth and bank erosion varied over the course of a hydrograph that included overbank flow. We hypothesized that variable discharge, in addition to sufficient bank strength, would lead to the successful modeling of a single-thread, laterally migrating channel. Specifically, we expected that overbank flows would provide sufficient flow depths to drive adequate bar growth, both laterally and vertically, thus balancing bank erosion and bar growth, and together produce lateral migration of the channel. We additionally explored how our model channel would respond to the different hydrograph components (the rising limb, peak, and falling limb) by quantifying the changes in sediment storage, rates of deposition and erosion, and channel cross-section and planform geometry. In this paper, we present results from three experimental runs conducted using a single-bend model channel, one initial condition run and two variable flow runs having an identical hydrograph shape. The purposes of the two hydrographs were to: 1) simulate a “realistic” high flow event; 2) increase flow depths to drive vertical accretion of the bars up to the floodplain elevation; 3) drive lateral migration of the channel; and 4) quantify morphologic response to the continuous change in discharge.

## FLUME BASIN EXPERIMENTS

### Experimental design

We carried out our experiments at the hydraulics laboratory at the University of California at Berkeley's Richmond Field Station. We used a 6.1 m long by 3.7 m wide flume basin set to a slope of 0.5% (Figure 1). The water was re-circulated through the system and sediment was fed at the upstream end of the flume and collected in a trap at the downstream end of the flume. The water and sediment entered a fixed channel entrance box set at a 15-degree angle to the longitudinal axis of the flume. A perforated screen across the downstream portion of the basin acted to support the floodplain material and allow the groundwater to pass through. The screen height was set below the floodplain at the elevation of the channel bed. An instrument carriage with topographic survey equipment could be moved above, and along a plane parallel to, the floodplain surface.

Our model channel was not a replication of any prototype river, but rather the experimental parameters (discharge, sediment size distribution and feed rates, channel geometry, and floodplain slope) were scaled together by means of undistorted geometric and Froude-scale modeling using the methods outlined by *Parker et al.* (2003) (Table 1). This method allowed us to model a flood event and the resulting channel response via processes such as bar growth and bank erosion within a period of hours rather than days, as would be expected in a natural river system. Assuming a model to prototype scale ratio of 1:40, our 0.5 m wide channel would be equivalent to a 20 m wide river. Time was additionally scaled in our experiments where, using the same example scale ratio, an hour in our model would represent approximately 6.3 hours in the prototype. All parameters were scaled to the median grain size of the bed and floodplain sediments. The median grain size was selected iteratively so that the channel could fit within the flume basin. The channel parameters were gradually refined during our preliminary experimental runs; the details of the preliminary runs are briefly summarized below, in the results section of this paper.

The floodplain and bed material was well-mixed sand (model gravel) and ranged in sizes from 0.2 to 3 mm, with a median size of 1 mm (Figure 2). The bed surface grain size distribution was allowed to evolve freely during the experiments. Initially, the floodplain was made planar with a uniform depth of 10 cm. A single-bend, rectangular channel with low sinuosity and constant width, depth, and planform curvature was carved into the floodplain. The sinuosity was 1.01 and radius of curvature was 21 m. The initial channel width and depth were 50 cm and 1.7 cm, respectively, giving a width to depth ratio of 30. The entrance and exit of the channel were situated at the cross-overs that bounded the single bend.

To add strength to the bank material, we applied a thin (~1 mm) layer of fine, ground silica and grew alfalfa sprouts (*Medicago sativa*) uniformly on the floodplain. The silica sizes ranged between 2 and 90  $\mu\text{m}$ , with a median size of 27  $\mu\text{m}$  (Figure 2). The effects of alfalfa in enhancing bank strength in non-cohesive sediments have been successfully demonstrated in similar modeling experiments (*Gran and Paola, 2001; Tal and Paola, 2007*). Along natural rivers with vegetated banks, the tensile strength and dense network of the root structures increases soil strength (*Thorne, 1990*). We observed that the sprouts physically adhered to the sediment grains which were qualitatively determined to provide effective cohesion to the floodplain and banks (Figure 3). We also observed that decaying sprouts on the floodplain provided a sticky organic layer, or "bio-film" (*Parker, 2005, personal communication*), that further provided cohesion to the sediment grains. The sprouts typically grow about 5 cm above and 1 cm below the floodplain surface. During the experiments discussed in this paper, the alfalfa rooting depth ranged between 0.1 to 0.5 cm, which was considerably less than our preliminary experiments. The size and rooting depth of the alfalfa sprouts was a function of temperature and light availability, and thus varied depending on the season during which the experiments were conducted. Although not consistently quantified, and strongly spatially and temporally variable, the density of alfalfa rooted in the floodplain

was approximately five sprouts per cm<sup>2</sup>. Cohesion due to alfalfa roots of up to 11.8 kPa was measured by *Pollen and Simon* (2006) for densities of ten sprouts per cm<sup>2</sup>. We provided water to the sprouts continually between runs with a low flow through the channel at about one-tenth the discharge at which sediment transport begins. The channel form was not affected by these periods of very low discharge. We re-applied alfalfa seeds to the floodplain by hand following each run to replace any dying or displaced sprouts.

The experimental series of runs presented herein were part of Run Series 6 that followed five preliminary run sets. This series consisted of one initial condition run with steady discharge near bankfull (Run 6.1) and two hydrograph runs that peaked at twice bankfull discharge (Runs 6.2 and 6.3) (Table 2; Figure 4). The discharges required to initiate sediment transport ( $Q_{cr}$ ) and fill the channel up to bankfull ( $Q_{bf}$ ) were predicted before the experiments began. We determined  $Q_{cr}$  and  $Q_{bf}$  to be 1.0 and 2.2 L/s, respectively, by taking the product of channel width, depth, and the flow velocity, in which the velocity was calculated using the Manning's equation. We estimated the Manning's  $n$  value used in the velocity equation to be 0.015 during our preliminary experiments. The critical sediment transport depth used to calculate  $Q_{cr}$  was selected iteratively by determining the depth required to make the Shields parameter ( $\tau^*$ ), or dimensionless critical shear stress for  $D_{50}$ , exceed the critical Shields parameter ( $\tau^*_{cr}$ ) for onset of sediment motion:

$$\tau^*_{cr} = \frac{\tau_b}{(\rho_s - \rho_w)gD_{50}} = \frac{\rho_w g h S}{(\rho_s - \rho_w)gD_{50}} \quad (1)$$

where  $\tau_b$  is the boundary shear stress at the threshold of motion,  $\rho_s$  is the sediment density measured to be 2,667 kg/m<sup>3</sup>,  $\rho_w$  is the fluid density,  $g$  is gravity,  $h$  is flow depth which may be substituted for the hydraulic radius for wide channels, and  $S$  is the channel slope. We had previously estimated  $\tau^*_{cr}$  to equal 0.03 for the median grain size of our floodplain and channel sediments, which is an expected value for quartz-based sand (e.g., *Julien, 1998*).

The sediment feed rate that would balance the sediment transport capacity was calculated using a one-dimensional sediment transport model and assumed that the average flow depth could be calculated using the Manning's equation for a rectangular channel (Table 2; Figure 5). The sediment feed rate at each discharge was determined using our predicted stage-dependent, channel boundary shear stress with a modified one-dimensional transport equation of Meyer-Peter and Müller by *Wong and Parker* (2006b), which is considered appropriate for wide channels:

$$q^* = 3.97(\tau^* - \tau^*_{cr})^{3/2} \quad (2)$$

where  $q^*$  is the dimensionless sediment transport rate. We found that equation 2 worked well using  $\tau^*_{cr}$  to equal 0.03 for the median grain size of our floodplain and channel sediments. This model assumes that the channel depth is uniform, which is not the case for our flume, but our preliminary experiments indicated that it accurately predicted sediment flux in our channel.

The sediment fed into the channel was intended to move as bedload only. We did not feed any suspended sediment during the experiments presented here based on problems created by their use during our preliminary runs. For example, some of the fine ground silica ( $D_{sil50} = 27 \mu\text{m}$ ), which we supplied to serve as suspended load, settled out and buried the predominately bedload-dominated channel bed. This outcome was similar to *Schumm and Khan's* (1972) experiments, and effectively prevented entrainment of the coarser bed material. To compensate for the lack of suspended sediment feed in the subject runs, we used a bedload grain size distribution that was slightly finer than the distribution of the floodplain

sediments (Table 2; Figure 2). These sediments ranged in sizes from 0.1 to 3 mm, and had a median diameter ( $D_{bf50}$ ) of 0.8 mm. We used a fine, unimodal white sand, with a  $D_{50}$  of 0.17 mm, for the finest fraction of the bedload distribution. This sediment provided an added benefit during the experiments as we were able to visually monitor its movement and deposition on the channel bed because its color made it clearly distinguishable from the remainder of the channel and bedload feed sediments.

The purpose of Run 6.1 was to allow bar-pool topography to form within the rectangular-carved channel without any channel expansion through bank erosion. We verified the predicted value for  $Q_{cr}$  as we slowly increased the flow over the initial 2.5 hours of the run (Figure 4). Initial sediment transport on the channel bed preceded sediment feed into the channel by an hour. Once the discharge reached 2.0 L/s, and was just below bankfull depth, the discharge and sediment feed rate were held constant for five hours. The hydrograph pattern used during Runs 6.2 and 6.3 was designed to resemble a natural, flood hydrograph characterized by a steep rising limb, a peak, and a decaying falling limb. The discharges ranged between  $Q_{crit}$  and two times  $Q_{bf}$  (“ $2Q_{bf}$ ”), with a mean of 2.0 L/s, slightly below  $Q_{bf}$ , over the hydrograph run duration. The rising limb increased at a constant rate while the falling limb had an exponential decay constant of approximately -0.3/hr. The hydrograph was divided into seven steps of constant discharge. The rising limb and overbank steps, Steps 1 through 5, each had durations of 30 minutes (150 minutes total). The falling limb steps, Steps 6 and 7, were 90 and 150 minutes in duration, respectively (240 minutes total). The flume was turned off at the end of each step in the hydrograph to collect the sediment accumulated in the trap at the downstream end and to survey the topography of the floodplain and channel. To resume the subsequent hydrograph step, we slowly increased the discharge and sediment feed over the first few minutes to avoid sudden sediment transport involving either bank failure, bed incision, or initiation of a sediment wave along the bed.

### **Quantifying channel response**

We made detailed measurements of the developing channel during and between each hydrograph step. Topographic surveys of the evolving channel surfaces were conducted prior to the initial experimental run (Run 6.1) and following each step. The surveys utilized a laser-line photogrammetry technique that consisted of capturing a series of regularly-spaced, obliquely-orientated digital images of a vertical laser-line projected onto the channel and floodplain surface perpendicular to the basin’s long axis (*e.g.*, Johnson and Whipple, 2007; Rowland, PhD diss., 2007). The spacing of the images along the basin was 5 cm. Once the images were corrected for perspective distortion, the cross-sections extracted from the laser-lines were combined to create a topographic surface, 5.15 m in length by 1.64 m in width, with an accuracy of  $\pm 1$ mm in each x-, y-, and z-direction.

We compared the topographic surfaces from each discharge step and also extracted five cross-sections from the surface, which were orientated normal to the flow and remained in that orientation throughout all three runs (Leverich, 2006). Data from the middle three cross-sections (XS 1.5m, XS 2.5m, and XS 3.5m), located within the channel bend, are presented in this paper (Figures 6 and 7).

Water surface slope and flow depth were measured with a point-gage at six evenly-spaced points along the basin’s long axis. Three of these point locations intersected the mid-points of the cross-sections (XS 1.5m, XS 2.5m, and XS 3.5m). The water surface slope was calculated using data from all six points and then used to measure the variations in the depth-averaged, boundary shear stress in response to the discharge per step and the evolving channel form (Table 2). The water surface elevation data were joined with the topographic survey data at the three cross-sections in order to relate the water surface elevation with the corresponding channel surface topography for each hydrograph step (Figure 7). We additionally monitored flow conditions with water surface velocity measurements twice per hydrograph step. Velocity was measured using a float and a stopwatch and then multiplying the values by 0.8 to convert to the mean depth-average velocity (Leopold *et al.*, 1964) (Table 2).

We calculated a mass balance of sediment for each discharge step by subtracting the outgoing sediment from the sediment fed into the channel. We collected the outgoing sediment at the downstream end (Figure 1) using a removable, screened basket that captured all grains larger than the  $D_{10}$  of the feed distribution and the  $D_5$  of the floodplain and initial channel sediment distribution. The basket was emptied at the end of each run step and the collected sediment was dried and weighed to determine the mass flux-out per step. The accuracy of the sediment weight measurements was  $\pm 0.05$  grams.

The topographic survey was augmented with overhead photographs taken once per minute to document channel changes over shorter time scales. The images were compiled and used to create a time-lapse movie that provides a view of the evolution of the channel morphology during the entire run (see flume experiment movies at: <http://flume.stillwatersci.com>).

## RESULTS

### Preliminary experiments

We conducted several preliminary experiments prior to the experimental runs presented in this paper, which we used to refine the many parameters of our experimental design, including grain size, sediment feed rates, floodplain slope, channel geometry, and bank strength. During our initial experiments, the use of coarser sediments ( $D_{50}=2$  mm) and a lack of bank strength quickly resulted in channel widening, aggradation, and development of a multi-channel pattern, which indicated that the materials were too coarse and bank strength too weak to control channel widening. In order to limit the amount of sediment originating from eroding banks and to estimate  $\tau_{cr}^*$ , we experimented within a sinuous channel bounded by fixed walls. We qualitatively confirmed that alfalfa grown on the narrow floodplain sections between the channel banks and the fixed walls slowed bank erosion rates and promoted overbank deposition of fine bedload and suspended load sediments through a reduction of local flow velocities.

The channel was free to evolve within the entire basin during the next phase of experiments, which maintained the same experimental conditions used during the fixed-wall experiments. A straight channel with one bend located at the channel entrance was initially carved into the floodplain and eventually two additional bends developed downstream. While the channel migrated through the floodplain, we observed that erosion rates were inversely proportional to alfalfa sprout density, which has been observed along natural banks as well (e.g. Thorne, 1990; Simon and Collison, 2002; Micheli et al., 2004). This indicated that the alfalfa were providing some degree of bank strength to the non-cohesive floodplain materials. The discharge was held at bankfull resulting in self-formed bar-pool topography, however, the bars remained separated from the inner banks by chutes that continued to convey water, but not sediment, throughout the experiments. We supplied both bedload and suspended load sediment. The suspended fines eventually coated the channel which essentially prevented all bed material entrainment (Schumm and Khan, 1972). The channel sinuosity progressively increased and eventually several cut-offs developed as the main flow path re-occupied the chutes that had separated the bars from the inner banks. The mechanism responsible for forming the cut-offs appeared to be related to the lowering of the bed elevation as the bedload feed was stopped and several knick-points, or head-cuts that formed downstream, advanced upstream through the chutes. Head-cuts only developed after suspended sediments had been fed into the channel and accumulated onto the bed surface.

Hydrographs and discharge-dependent sediment feed rates were introduced in later experimental runs, however, although channel sinuosity and cut-offs developed, problems with suspended sediment deposition, bed aggradation, and disconnected point bars continued. In response, we made several adjustments to our experimental design for the subject experimental runs of this paper. First, we lowered the floodplain slope from 1% to 0.5% in the expectation that bar growth would be enhanced (Parker,

2005, pers. comm.). Second, the bedload size distribution was slightly fined to have a median diameter of less than 1 mm. Third, we did not feed any suspended sediments to avoid causing the problems discussed above. Instead, we applied the fine silica directly onto the floodplain to enhance bank strength.

## **Hydrograph experimental runs**

### *Morphologic development*

During the course of the three experimental runs a bar-pool topographic feature formed within our model channel (Figures 6 and 7). The channel developed a point bar, located along the inside of the bend, and a thalweg and near-vertical cut-banks along the outside of the bend. This topography initiated during the Run 6.1 (the initial condition run with discharge greater than critical but slightly below bankfull), in the form of two alternate point bars that were separated from the floodplain by a narrow chute (Figure 6b). The topography resulted from scouring along the thalweg (*i.e.*, pool formation) and vertical bar growth up to two-thirds of the bank height, as shown at cross-section XS 1.5m in Figure 7a. The chute between the bar and the inner bank represents the lack of sediment delivery at the inner bank toe. This feature is similar to the chutes that developed during our preliminary runs and to those of other experimental studies (*e.g.*, Friedkin, 1945; Schumm and Khan, 1972; Eaton and Church, 2004).

No bank erosion occurred during this run, which indicated that the bank strength exceeded the applied shear stresses under the imposed flow regime and sediment feed rate (Figures 6b, 7a). This was a desired outcome since it was our intention to promote bar-pool development in the absence of bank erosion, thus avoiding channel widening due to an imbalance between outer bank retreat and inner bank advancement. Despite the lack of outer bank migration, the channel cross-section form was adjusted by the bar growth and pool scour over the course of this run. A predominant lateral adjustment of the channel's centroid, which responds to a combination of bank erosion and topographic change between both banks, thus resulted. The ratio of vertical to lateral change in centroid position was 1:58, indicating that the channel shifted laterally much more than it shifted vertically.

During the first hydrograph run (Run 6.2), the morphologic response was minimal during the first step at  $Q_{cr}$ , but there was bedload transport along the thalweg (Figure 7b). Some vertical bar growth and deposition in the pool and chute occurred during Step 2 at  $Q_{bf}$ , but the bar remained disconnected from the inner bank and erosion of the outer bank was very small. Similar to the bar growth dependence on flow depth in Run 6.1, the bar top grew vertically but no closer than approximately 0.5 cm of the water surface elevation. During the first overbank flow step, Step 3 at  $1.5Q_{bf}$ , the bar continued to grow, the chute filled in significantly, and bank erosion shifted the outer bank position laterally by 1.7 cm (Figure 7b). We observed that fine bedload was transported over the upstream bar portion into the chute, and then proceeded to move longitudinally down the chute during the three overbank flow steps (Steps 3, 4, and 5). Sediment transport into and within the chute ceased at the completion of the overbank flow steps and ultimately one-third of the bar length connected to the inner bank (Figure 6c). The outer bank proceeded to erode along the length of the channel bend, but with a stronger focus opposite to the upstream portion of the bar that first accreted to the floodplain elevation and connected to the inner bank (XS 1.5m). The bank erosion continued well into the falling limb steps at  $Q_{bf}$  and  $Q_{cr}$  only along the banks at this location (Figure 7b). Channel adjustments at this cross-section were significantly greater in the lateral direction; the ratio of vertical to lateral centroid change was 1:860 over the run duration.

In Run 6.3, the lateral channel migration continued in response to another round of overbank discharge (Figure 6d). The bar continued to accrete vertically, filling in a small trough-shaped depression that had formed during the falling limb of Run 6.2, and the bar top at the elevation of the floodplain advanced in the direction of outer bank migration (Figure 7c). At cross-section XS 1.5m, the bar top laterally advanced 9.5 cm towards the outer bank and nearly kept pace with the outer bank migration, which advanced 12 cm. These two values respectively represent 19% and 24% of the initial channel width

( $W=50$  cm). The movement of the centroid at the start and end of the run indicates a vertical to lateral adjustment ratio of 1:48, which is substantially less than the adjustment ratio during the previous run. This lower ratio was driven by the net rise of the minimum bed elevation (Figures 7b and 7c). During both hydrograph runs, the minimum bed elevation fluctuated with the rise and fall of discharge. The bed elevation at the end of Run 6.2 was less than at the start resulting from the continued bank erosion and pool scouring throughout the falling limb steps (Figure 7b). However, during Run 6.3, the pool filled returning the minimum bed elevation to within nearly 0.1 cm (about 1 median grain size) of the mean value of the three runs.

The hydraulic parameters measured during the experiments, including water surface slope ( $S_{ws}$ ) and depth-average flow velocity ( $\bar{u}$ ), tracked the discharge (Table 2). The channel width progressively increased over the course of all three runs. During both hydrograph runs, we observed the banks to erode by individual grain entrainment. The fine silica layer and sprouts on the floodplain and bank tops eroded and fell into the channel once they had been undercut. These pieces of eroded floodplain surface were quite small ( $<1$  cm<sup>2</sup>) and quickly ( $<60$  seconds) disintegrated in the main flow path. Bedload transport and bed material entrainment spanned nearly the entire channel width during most of the discharge steps, even at  $Q_{cr}$ , with increased transport rates driven by the magnitude of flow. Grain sorting was observed across the face of the bar where the finest size fractions moved and deposited within the shallowest portions of the channel including the chute (Figure 8). Several bedforms developed, including ripples and dunes, where their presence and relief were observed to be dependent on flow intensity associated with water surface waves. Additionally, features resembling scroll bars were along the downstream end of the bar, with individual scrolls associated with different discharges, and lateral motion of the bar (Figure 6d).

#### *Sediment transport*

There was a net accumulation of sediment within the channel over the course of the three experimental runs, however, nearly 100% of the accumulation occurred during the initial run (Run 6.1) when bar growth first occurred (Table 2; Figure 5). The total mass of sediment fed into the channel during the three runs was 84 kg, while the total mass out was 71 kg. This resulted in a positive balance of 13 kg, or 15% of the total flux in. During Run 6.1, an accumulation of 14 kg of sediment occurred which contributed to the bulk of the main point bar. Relatively small changes in the net sediment storage occurred over the course of each of the two hydrograph runs, indicating a relative mass balance: -2.4 kg and 1.5 kg, which respectively accounted for 8% and 5% of the total mass fed per run. There were, however, variations between the sediment input and output transport rates during each of the two hydrograph runs that caused temporary disequilibrium in the mass balance (Figures 5a and 5b). During the three overbank flow steps (Steps 3, 4, and 5), the input rates exceeded output rates resulting in a net accumulation of sediment. The opposite occurred during the  $Q_{bf}$  steps (Steps 2 and 6) where output rates exceeded input rates, but with greater differences during the falling limb step (Step 6). Output rates were greater during Step 6 rather than being equal to or greater than output rates during Step 2 due to a sediment conveyance time lag within the channel as the sediment mass fed into the channel during the relatively short overbank flow steps continued to transport out of the channel well into the subsequent run steps (*i.e.*, Step 6). Although the highest output rates occurred during the peak step (Step 4), the greatest proportion of the total mass of sediment transported out of the channel consistently occurred during the  $Q_{bf}$  step on the falling limb (Step 6), where the time duration was equal to the combined overbank flow step durations. The differences between input and output rates during the  $Q_{cr}$  steps (Steps 1 and 7) were relatively minor and insignificantly affected the long-term mass balance.

The grain size distributions of the sediment flux-out varied only slightly between each run step and did not vary consistently with discharge (Table 2; Figure 9). The maxima to minima range of the grain size distributions of the initial run (Run 6.1) and the 14 hydrograph steps is shown in Figure 9. The  $D_{50}$  of each of the transported size distributions ( $D_{out50}$ ) ranged between 0.6 and 0.9 mm, and were similar to  $D_{bf50}$  (0.8 mm) and slightly finer than  $D_{fp50}$  (1 mm). The  $D_{84}$  of the transported material size distributions

( $D_{out84}$ ) ranged between 1.3 and 1.5 mm and were consistently finer than the  $D_{84}$  of the bedload (1.8 mm) and floodplain (1.9 mm), which indicates that a portion of the coarse fraction of sediment entering the channel, from either the bedload feed or the floodplain, was retained. The  $D_{16}$  of the transported material size distributions ( $D_{out16}$ ) ranged narrowly between 0.3 and 0.4 mm and were bounded by the  $D_{16}$  of the bedload (0.2 mm) and floodplain (0.4 mm).

### **Rates of deposition and erosion in cross-sectional areas**

The rates of total deposition and total erosion at three cross-sections, defined by the change in area per step duration, generally trended with the discharge during the two hydrograph runs (Figure 10). The maximum rates of total deposition and total erosion at each cross-section occurred during one of the three overbank flow steps during Run 6.2, but the maximum was not necessarily at the highest peak (Figure 10a). The same occurred during Run 6.3, except at XS 1.5m where the total erosion rate reached a maximum value during the first  $Q_{bf}$  step (Step 2). The magnitude of total deposition and total erosion rates were consistently greater during Run 6.3 in comparison with Run 6.2 at all three cross-sections, but even more so at XS 2.5m and XS 3.5m. During Run 6.2, the two greatest rates of total deposition and total erosion occurred during the peak step and were 24 (XS 1.5m) and 19  $\text{cm}^2/\text{hr}$  (XS 2.5m), respectively. In contrast, during Run 6.3, the greatest rates were 48 ( $2Q_{bf}$ ) and 50  $\text{cm}^2/\text{hr}$  ( $1.5Q_{bf}$ , Step 3), respectively, and both occurred at the bend apex at XS 2.5m.

Through isolating areas of the cross-sectional areas that are shaped by specific channel processes—bar growth, pool fill, bank toe fill, bank erosion, pool scour, and bar loss—we found that their individual rates of change also generally tracked discharge (Figure 10). This analysis was motivated by a need to follow the changes of specific channel processes, such as bar growth and bank erosion, which do not always make up the entirety of the total deposition and total erosion, respectively. This is because, with temporary vertical variations, deposition can occur in the pool separate from bar growth and erosion can occur on the point bar separate from bank erosion, which is not incorporated in the classic view of a laterally migrating channel over the long-term (e.g., *Leopold et al.*, 1964; *Knighton*, 1998). The purpose of this analysis was therefore to attribute the proper morphologic processes to the changes in channel form between successive cross-sections. Although some previous field studies have defined fluvial landforms at a cross-section in order to quantify changes in area (e.g., *Andrews*, 1982; *Anthony and Harvey*, 1991), there is little agreement in those definitions and not all features, such as terraces and benches (*Pizzuto*, 1994), were present in our model channel. Therefore, we have defined the component areas contributing to the total deposition area as bar growth, pool fill, and bank toe fill, while the component areas that contributed to the total erosion area were defined as bank erosion, bar loss, and pool scour (Figure 11).

In our analysis, we found that bar growth was the dominant contributor to total deposition during both hydrograph runs at all three cross-sections, accounting for more than 75% of the total deposition during six out of seven steps of each hydrograph run (Figures 10a, 10b, and 10c). This indicates that the focus of deposition in the channel was on the point bar, as opposed to within the thalweg as either pool fill or bank toe fill. An exception occurred at XS 3.5m during Step 3 ( $1.5Q_{bf}$ ) and Step 4 ( $2Q_{bf}$ ) of Run 6.3 where the greatest contribution to the total deposition was from bank toe fill and pool fill, respectively, indicating that deposition was momentarily greater along the thalweg, or pool, in this portion of the channel (Figure 10c). The dominant components contributing to the total erosion alternated between bank erosion and bar loss. The total erosion was dominated by pool scour during only two steps of the runs: Step 3 of Run 6.2 at XS 2.5m and Step 2 of Run 6.3 at XS 3.5m (Figures 10b and 10c). In those cases where bank erosion was the dominant contributor, it often exceeded bar loss and pool scour combined by a factor of 10 and did so most often during the peak steps. During the  $Q_{cr}$  steps, the majority of total erosion was contributed by bar loss, except at XS 1.5m during the last step of Run 6.2 and the first step of Run 6.3 where bank erosion dominated, albeit at relatively low values. This indicates that bank erosion generally

accounted for a comparatively small portion of the total erosion during low discharges while representing a significant contribution during the peak flows.

In our analysis comparing the rates of total deposition and total erosion as a function of discharge, there was no trend in their ratio plotted against discharge at the three cross-sections (Figure 12). The ratios were generally near unity when considering all cross-section data. Individual cross-sections exhibited some patterns during both hydrograph runs, such as XS 3.5m where total deposition rates were consistently greater than total erosion rates during  $Q_{cr}$  of both hydrograph runs. However, the general trend among the data from each cross-section reveals an inconsistent dependence on discharge, as further supported by differences in ratio values at a given discharge. The hysteresis behavior was also inconsistent as the direction was neither clockwise nor counter-clockwise for all cross-section data. Additionally, although not presented in detail here, the relationship between bar growth rates and bank erosion rates was analyzed and similarly exhibited no dependence on discharge (Leverich, 2006). These results were all strongly influenced by the rates of sediment fed into the channel, which we controlled with the goal of maintaining a balance between deposition and erosion, thus minimizing the potential for either deposition or erosion at a cross-section to exceed the other.

In general, the total deposition and total erosion rates were both greater during the rising limb than the falling limb, especially at the  $Q_{cr}$  step (Figure 13). Although the rates of channel change were generally greater during the rising limb at the lowest discharge, closer to the peak step the rates of channel change were greater during the rising limb near the upper portion of the channel bend (*i.e.*, XS 1.5m). In contrast, the rates of channel change were greater during the falling limb, or are very close to unity, near the lower portion of the channel bend (*i.e.*, XS 3.5m). This indicates a time lag along the channel length where the rates of channel change nearer to the channel origin are greater earlier in the hydrograph while rates of channel change farther downstream became greater later in the hydrograph. During Run 6.3, the total deposition and total erosion rates were consistently greater during the two steps following the peak step along the falling limb at XS 3.5m (Figures 13b and 13d). We attribute this to the migration of the bend apex—the focus of maximum channel migration—towards this portion of the channel after the peak step. The one exception to the trend of greater rates of channel change during the rising limb at the lowest discharge was at XS 1.5m during Run 6.2 where erosion rates were greater during the falling limb (Figure 13c). As explained above, this resulted from an increase in bank erosion and pool scour rates through every step of the falling limb at the bank position opposite to the newly-developed, and connected, point bar (Figure 7b).

## **DISCUSSION**

The channel morphology that developed during the three runs, including bar-pool topography and cut-banks, indicates that our experimental goal to model a single-thread, meandering floodplain channel, while testing the effects of flood hydrographs, was achieved. The channel-forming processes that contributed to the resultant morphology in our model also occur in natural rivers, including bed load transport and sorting, bar growth, bank erosion, lateral migration, and pool fill and scour. Additionally, the channel exhibited neither net aggradation nor incision as a result of achieving near-equilibrium between the sediment flux in and out during the two hydrograph runs. This indicates that: 1) the sediment input rates were scaled appropriately to the discharge based on the expected shear stresses within the channel; and 2) there was a balance between deposition within the channel via bar growth and erosion from the banks after the initial run (Run 6.1). Our modeling approach may therefore serve as a tool for future river restoration design based on the morphology and active processes that developed within the channel that are similar to those occurring within a natural river.

In our two hydrograph runs, it was clearly shown that the crucial experimental condition required to drive the lateral migration of the channel while maintaining a relatively stable width, single thread channel was the inclusion of overbank flows. The overbank flows provided sufficient flow depths to build the well-formed point bar, whereby the finer size fraction of the mixed bedload material could be transported and deposited upon the bar. The main point bar was thus allowed to vertically accrete to the floodplain height and, through the filling of the chute, became completely connected to the inner bank along the upper third of the bar's total length. This process has been documented in the field by *Anthony and Harvey (1991)* who observed bar heights to increase via deposition during flows greater than bankfull. In our model channel, the overbank flows also drove erosion of the outer bank by providing shear stresses in excess of the resisting bank strength. Together with the lateral migration of the inner bank, the channel laterally migrated through the floodplain while increasing only slightly in width. These developments support our hypothesis that overbank flows are a necessary experimental condition driving the lateral migration of the channel, by contributing to vertical bar growth and connection with the floodplain. Restoration planners seeking to restore the lateral migration process of a channel should explicitly consider overbank flows and design the channel for a given flood frequency in order to ensure occasional overbank flow events.

The formation of a point bar that served to laterally advance the inner bank in the direction of channel migration was one of the most critical processes to model in our experiments. We infer, based on previous modeling experiments (*e.g., Friedkin, 1945; Schumm and Khan, 1972; Eaton and Church, 2004*) and our own preliminary experimental runs, that if the bar had remained submerged and disconnected from the floodplain during our experiments, the channel would have become progressively wider to the point where net aggradation of the channel bed could have occurred, thus leading to a braided channel form. The final bar form that developed, therefore, represents a significant advance in the modeling of meandering channels, as bar-connection to the floodplain has been the primary deficiency in previous modeling experiments, and thus further justifies using our modeling approach for guiding river restoration designs.

In addition to providing overbank flow, the bar growth process was aided by the availability of finer bedload grains that were selectively transported upon the bar top and within the chute (Figure 8). Although the chute did not fill along the entire bar length, we can surmise that the chute would have continued to fill if suspended sediments had been fed in addition to the bedload. The suspended sediments would have had the benefit of requiring shallower flow depths (*i.e., less shear stress*) to be transported and deposited upon the bar top and within the chute in comparison with the relatively less mobile bedload grains. Restoration planners designing for active point bar growth within a stream channel should therefore not only consider the flood frequency of overbank flows that will carry sediment up to bar tops and within chutes, but also the availability of fine bedload and suspended load sediments that can be more easily transported and deposited to those shallower portions of the channel.

Planners seeking to accelerate restoration efforts could additionally construct the point bars as part of the channel reconstruction efforts which, like our model channel, are seldom included in favor of allowing bars to develop freely (*i.e., un-aided*) within a channel with uniform width and depth. During a field experiment that deliberately altered the cross-sectional morphology of a small stream in North Carolina in order to systematically force flow convergence and divergence, *Keller (1978)* demonstrated that bar growth was favored along the lower gradient bank of a channel segment that had been given an asymmetrical cross-section. The bars quickly emerged during the first flood event and remained stable during several additional floods. Application of a bar-promoting method akin to this one could potentially minimize the development of un-desired morphology, such as submerged and disconnected point bars, net bed aggradation, or a braided planform, especially where strict flow regulation and insufficient sediment supply exists.

The strength of the outer banks was another key element of our experiments that helped maintain a single thread channel, by limiting bank erosion rates. The banks were, however, still erodible, leading to their gradual retreat, especially during the peak discharge. Lateral migration of the channel resulted with the simultaneous action of bank retreat and inner bank advancement as part of the bar building process. Although the rates of outer bank retreat slightly exceeded that of the inner bank advancement, which led to some channel widening, the bank strength provided by the alfalfa and fine ground silica on the floodplain appears to have been adequate for the purposes of these experimental runs. Their contributions to controlling the rates of outer bank retreat is further qualified by pointing out that the channel did not exhibit net aggradation or development of a mid-channel bar or braid planform, which often occurs during or soon after a channel has over-widened.

The process by which our model banks eroded, plucking of individual grains at the bank toe, is similar to that observed along natural non-cohesive banks (Thorne, 1982). One difference is that the eroding banks did not exhibit mass failures, such as calving or slumping, which could occur in restored channels depending on bank material composition. Initiation of bank erosion began in our experiment once the flow was above bankfull (Run 6.2, Step 3:  $1.5Q_{bf}$ ) and did not continue when the flow was equal to or less than bankfull, except at the bank portion near XS 1.5m during the falling limb steps of Run 6.2. Bank erosion driven by overbank flows was likely due to two mechanisms: 1) increased pore water pressure during bank and floodplain inundation; and 2) increased flow velocities, and thus shear stresses acting against the outer banks. The former mechanism could not be quantified since the bank strength was not measured; however, since there was similarity in the manner of bank erosion in our model and a natural channel, it can be safely inferred that increased pore water pressures decreased the bank stability when the banks were submerged during overbank flow (Thorne, 1982). The occurrence of the latter mechanism is supported by the increased shear stresses estimated within the channel during the overbank flow steps as driven by greater flow depths coupled with faster flow velocities (Table 2).

Based on the important role that bank strength played in controlling the width of our single-thread channel, restoration planners should therefore include this channel parameter into their designs to control erosion rates especially for banks predominately comprised of easily erodible, non-cohesive materials (e.g., sands and gravels). The degree of bank strength needed to control bank erosion rates, and yet allow for occasional migration, would need to be scaled to the flood frequency in order to maintain a balance between outer bank retreat and inner bank advancement over time. As our use of alfalfa demonstrated experimentally, riparian vegetation is an essential restoration tool for controlling streambank stability (e.g. Simon and Collison, 2002; Micheli et al., 2004).

The supply and size distribution of sediment that entered our model channel via bedload feed and eroding banks maintained the sediment mass balance within the channel and contributed to the bar building process. Downstream of large dams, river restoration planners face significant challenges in providing an adequate supply of sediment with a wide grain size distribution. Under sediment supply-limited conditions, erosion of the banks (and floodplain) may provide the primary sediment supply source. Restoration planners should therefore encourage bank erosion to not only promote the lateral migration of the channel, but also to supply sediment into the channel. Since this supply is dependent on the number of bends with eroding banks and the lateral extent to which the banks can erode within a given reach, a long reach and a wide, accessible floodplain will be essential to balance the sediment flux through the restored channel.

In addition to responding to the magnitude of the specific discharges used in the hydrograph runs, the channel morphology was also dependent on the durations of the individual hydrograph steps. The durations of the overbank flow steps were long enough to allow lateral and vertical bar accretion and bank erosion to occur, but were not too long as to lead to excessive channel widening and adaptation to a new effective bankfull discharge. This could have occurred because the rates of outer bank retreat were

greater than the rates of inner bank advancement during these steps. Additionally, given that the bed elevation rose and fell with the discharge, it is also possible that the degree of aggradation within the channel would have increased during longer overbank flow steps. Instead, the change in sediment storage remained near zero over the course of the two hydrograph runs, primarily due to the increased output rates during Step 6 ( $Q_{bf}$ ) of the falling limb. The relatively longer durations of this step and that of the following step provided ample time to convey sediment that had accumulated within the channel during the rising limb and peak steps, thus balancing the total input and output. This result should not be interpreted to suggest that the significant work achieved at bankfull discharge during the falling limb was due to the specific flow magnitude (*i.e.*, effective discharge), as the magnitude-frequency concept of *Wolman and Miller* (1960) may imply. But rather, the significant output rates during this step were due to the continued passage of the accumulated sediment after the peak step that was provided necessary time to transport out of the channel, regardless of the specific discharge. We would deduce that net sediment accumulation would have occurred if the durations of those two steps were the same as each of the preceding steps (0.5 hr). For application to restoration design, variable discharges including occasional overbank peak flows should be used to drive specific channel forming processes. For example, an infrequently used hydrograph with an overbank flow peak would aid vertical accretion of point bars, while a more frequent hydrograph with a bankfull peak would be used to mobilize the bed, but would avoid driving channel migration.

Rates of morphologic change in our model channel were not only controlled by the temporal variation in discharge and sediment input, but also depended on the specific position along the channel length, the moment in time during the hydrograph, and the antecedent conditions present at the beginning of each run. For example, the bank erosion rates were not uniform along the channel length, but varied spatially and temporally as the bend apex migrated downstream over the course of both hydrograph runs. Bank erosion initiated locally near XS 1.5m, where and when the point bar first accreted to the floodplain height and connected to the inner bank (Run 6.2, Step 3:  $1.5Q_{bf}$ ) (Figure 7), but erosion along the downstream portion of the outer bank did not significantly occur during this run. As a portion of the channel width became essentially blocked by the point-bar, the flow was re-directed away from the bar resulting in increased flow velocities within the thalweg and against the outer bank. The bank erosion created a local increase in the outer bank's curvature, forming the bend apex, which eventually migrated downstream during the subsequent run (Run 6.3) as the bar continued to accrete in this same direction. The migration of the bend apex towards XS 3.5m also explains the higher erosion and deposition rates after the peak step of Run 6.3 (Figure 13d) despite that erosion and deposition rates were generally greater during the rising limb for a given discharge at the three channel cross-sections (Figure 13).

Topographic steering around a bar has been colloquially referred to as “bar-push” and has been observed in other laboratory experiments (*e.g.*, *Whiting and Dietrich*, 1993) and in the field. In meander bends of the gravel-bedded River Endrick, *Bluck* (1971) found that the direction of meander migration was dependent on the direction of bar growth. The topographic steering of flow towards the outer bank upstream may have also been responsible for the bar disconnection downstream. As the outer bank continued to erode downstream, the main flow path was sufficiently far from the bar top and chute to be able to transport sediment to and connect the downstream portion of the bar to the floodplain. Scroll bars associated with transported sediment across the bar surface formed during the steps of Run 6.3 where the opposing outer bank continued to erode after the peak (Figure 6d). For this downstream portion of the bend, the main flow path transporting the bulk of the bedload was essentially pulled towards the outer bank through a process that can be referred to as “bank-pull”. The dynamics of upstream bar push and downstream bar pull together appear to drive bend migration both laterally and downstream. These observations suggest that restoration of active lateral migration will be less successful where attempts are made to control bank erosion rates with locally hardened banks because bank erosion and bar growth are linked longitudinally within and between meander bends.

## CONCLUSIONS

We have successfully created 1:40 scale physical model of a stable width, laterally migrating meandering channel. Essential components of our experimental approach include variable discharge with significant overbank flow, variable sediment supply at approximately the rate of bedload sediment transport capacity, and bank cohesion supplied by alfalfa and a floodplain cap of silica silt. Several conclusions, outlined below, can be drawn from our results that may help guide channel and floodplain design in large-scale river restoration projects.

1. The physical processes that control the morphodynamics of laterally migrating meandering rivers can be replicated at a laboratory scale, creating the potential for testing of site-specific restoration channel and floodplain designs.
2. Overbank flows may be essential for maintaining a stable channel width during lateral migration because they are a critical component in attaching the bar to the floodplain. Channel and floodplain restoration designs should take into account the frequency and magnitude of overbank flows and not rely on a single effective design discharge such as bankfull.
3. Bar growth is a key process for maintaining a stable width migrating channel and avoiding excessive widening and a shift to a braided planform. Vertical accretion to the floodplain elevation and filling of the upstream portion of the chute along the inner bank appear to require both overbank flow and a sufficient bedload sediment supply. We infer that filling of the downstream portions of the chute depends on a sufficient supply of finer sediments transported as bedload and as suspended load. Restoration designs that include careful grading of initial bar pool topography are likely to achieve more rapid development of desired channel morphologies.
4. Bank strength is a key parameter which can be controlled in restoration design through adjustment of the density of riparian vegetation. Bank strength needs to be sufficient to limit bank erosion rates to approximate the rates of lateral bar growth, but not so strong as to prevent lateral migration during overbank flows.
5. Assuring adequate sediment supply to drive lateral and vertical bar growth is a major constraint on restoring actively migrating meandering channels downstream of dams. Restoration designs should be based in part on estimates of upstream supply of both bedload and suspended load sediments. Successful restoration is more likely in long reaches with multiple meander bends because bank erosion upstream can provide sediment supply for bar growth downstream.
6. The shape of typical flood hydrographs is a potentially important restoration design parameter because of the role of recession limb duration in sediment transport and deposition in chutes behind bars. Ideally, physical reconstruction of channel morphology can be linked to design of hydrographs of flow releases from upstream dams to achieve an optimal balance between erosional and depositional processes during channel migration.
7. The dynamics of lateral channel migration include both a bar-push effect due to topographic steering in the upstream portion of a meander bend and a bank-pull effect downstream. This constrains the possibility for restoration designs that seek to prevent or limit bank erosion at specific locations with a meander bend. Restoration of stable-width, laterally migrating channels is most likely to be successful where wide floodplain surfaces are available for the channel to migrate across.

**Acknowledgements:** This work was part of the Stillwater Sciences project: Physical Modeling Experiments to Guide River Restoration Projects supported by CALFED Bay Delta Authority. We thank the National Center for Earth-Surface Dynamics (NCED) and the Scientific Advisory Panel (SAP): Gary Parker, Tom Lisle, Peter Wilcock, Scott McBain, and Kris Vyverberg for their guidance and support. Additional thanks to: Joel Rowland of UCB for photogrammetry technique assistance; Stuart Foster, John

Potter, and Neto Santana for flume construction; Leslie Hsu of UCB for fine sand supply; Kathleen Swanson of UCB for experimental assistance and fine-sediment size analysis; John Potter for bedload sediment sieving; Ray Pestrong and Jerry Davis of SFSU for thesis committee guidance; Marwan Hassan of UBC for sediment feed-rate advice; Michal Tal of UMN SAF for alfalfa guidance; and Charles Smith for river modeling inspiration.

## REFERENCES

- Ackers, P., and F. G. Charlton (1970), The meandering of small streams in alluvium, Report 77, Hydraulic Research Station, Wallingford, U.K., 78 pp.
- Andrews, E. D. (1982), Bank stability and channel width adjustment, East Fork River, Wyoming, *Water Resour. Res.*, 18, 1184-1192.
- Andrews, E. D. (1986), Downstream effects of Flaming Gorge Reservoir on the Green River, Colorado and Utah, *Geol. Soc. Am. Bull.*, 97, 1012-1023.
- Anthony, D. J., and M. D. Harvey (1991), Stage-dependent cross-section adjustments in a meandering reach of Fall River, Colorado, *Geomorphology*, 4, 187-203.
- Bluck, B. J. (1971), Sedimentation in the meandering River Endrick, *Scott. J. Geol.*, 7, 93-138.
- CALFED Bay-Delta Program (2000), Final Programmatic EIS/EIR Technical Appendix, Ecosystem Restoration Program Plan, Volume 2, Ecological Management Zone Visions, Sacramento, Calif.
- Clear Creek Restoration Team (2000), Lower Clear Creek floodway rehabilitation project, channel reconstruction, riparian vegetation, and wetland creation design document, prepared by McBain and Trush, Graham Mathews, and North State Resources, 75 pp.
- Collier, M., R. H. Webb, J. C. Schmidt (2000) Dams and rivers: A primer on the downstream effects of dams, *U.S. Geol. Surv. Circ.*, 1126, 94 pp.
- Doyle, M. W., E. H. Stanley, D. L. Strayer, R. B. Jacobson, and J. C. Schmidt (2005), Effective discharge analysis of ecological processes in streams, *Water Resour. Res.*, 41, W11411, doi:10.1029/2005WR004222.
- Eaton, E. C., and M. Church (2004), A graded stream response relation for bed load-dominated streams, *J. of Geophys. Res.*, 109, doi: 10.1029/2003JF000062.
- Friedkin, J. F. (1945), A laboratory study of the meandering of alluvial rivers, *U.S. Waterways Experimental Station Report*, U.S. Army Corps of Eng., Vicksburg, MS, 40 pp.
- Graf, W. H., and Z. Qu (2004), Flood hydrographs in open channels, *Water Manage.*, 157, 45-52.
- Graf, W. L. (2005), Geomorphology and American dams: The scientific, social, and economic context, *Geomorphology*, 71, 3-26.
- Gran, K. and Paola, C. (2001), Riparian vegetation controls on braided stream dynamics, *Water Resour. Res.*, 37, doi: 10.1029/2000WR000203.
- Hassan, M.A., Egozi, R. and Parker, G. (2006), Experiments on the effect of hydrograph characteristics on vertical grain sorting in gravel bed rivers, *Water Resour. Res.*, 42, W09408, doi: 10.1029/2005WR004707.
- Jin, D., and S. A. Schumm (1987), A new technique for modeling river morphology, in *International Geomorphology, Part I*, edited by Gardiner, V., pp. 681-690, John Wiley & Sons, Chichester, U.K.
- Johnson, J. P. and K. X. Whipple (2007), Feedbacks between erosion and sediment transport in experimental bedrock channels, *Earth Surf. Processes Landforms*, 32, doi: 10.1002/esp.1471.
- Julien, P. Y. (1998), *Erosion and sedimentation*, 280 pp., Cambridge University Press, New York.
- Keller, E. A. (1978), Pools, riffles, and channelization, *Environ. Geol.*, 2, 119-127.
- Knighton, D. (1998), *Fluvial forms and processes*, 383 pp., Arnold Publishers, London.
- Kondolf, G. M., M. W. Smeltzer, and S. Railsback (2001), Design and performance of a channel reconstruction project in a coastal California gravel-bed stream, *Environ. Manage.*, 28, 761-776.
- Leopold, L. B. and M. G. Wolman (1960), River meanders, *Geol. Soc. of Amer. Bull.*, 71, 769-794.

- Leopold, L. B., M. G. Wolman, and J. P. Miller (1964), *Fluvial processes in geomorphology*, 522 pp., Dover Publications, Inc., New York.
- Leverich, G. T., 2006. The effect of variable discharge on the morphology of a model meandering river. M.S. Thesis, Department of Geosciences, San Francisco State University, 200 pp.
- Ligon, F. K., W. E. Dietrich, and W. J. Trush (1995), Downstream ecological effects of dams, *Bioscience*, 45, 183-192.
- McBain, S., and W. Trush (1997), The fluvial geomorphology of the Tuolumne River: implications for the riverine ecosystem and salmonid restoration, International Association for Hydraulic Research, International Association for Hydraulic Research, p. 569-574.
- Micheli, E. R., J. W. Kirchner, and E. W. Larsen (2004), Quantifying the effect of riparian forest versus agricultural vegetation on river meander migration rates, central Sacramento River, California, USA, *River Res. Applic.*, 20, 537-548.
- Palmer, M. A., E. S. Bernhardt, J. D. Allan, P. S. Lake, G. Alexander, S. Brooks, J. Carr, S. Clayton, C. N. Dawm, J. Follstad Shah, D. L. Galat, S. G. Loss, P. Goodwin, D. D. Hart, B. Hassett, R. Jenkinson, G. M. Kondolf, R. Lave, J. L. Meyer, T. K. O'Donnell, L. Pagano, and E. Sudduth (2005), Standards for ecologically successful river restoration, *J. of Applied Ecology*, 42, 208-217.
- Parker, G., C. M. Toro-Escobar, M. Ramey, and S. Beck (2003), Effect of floodwater extraction on mountain stream morphology, *J. Hydraul. Eng.*, 129(11), 885, doi:10.1061/(ASCE)0733-9429(2003)129:11(885).
- Peakall, J., P. J. Ashworth, and J. L. Best (2007), Meander-bend evolution, alluvial architecture, and the role of cohesion in sinuous river channels: A flume study, *J. of Sedimentary Res.*, 77, doi: 10.2110/jsr.2007.017.
- Pizzuto, J. (1994), Channel adjustments to changing discharges, Powder River, Montana, *Geol. Soc. Am. Bull.*, 106, 1494-1501.
- Pollen, N. and A. Simon (2006), Geotechnical implications for the use of alfalfa in experimental studies of alluvial-channel morphology and planform, *Eos Trans. AGU*, 87(52), Fall Meet. Suppl., Abstract H21G-1455.
- Power, M. E., A. Sun, G. Parker, W. E. Dietrich, and J. T. Wootton (1995), Hydraulic food-chain models, *BioScience*, 45, 159-167.
- Rowland, J. (2007), Tie channels, Ph.D. dissertation, 176 pp., Univ. of Cal. at Berkeley, Berkeley, Spring.
- Schumm, S. A., and H. R. Khan (1972), Experimental study of channel patterns, *Geol. Soc. Am. Bull.*, 83, 1755-1770.
- Simon, A. and A. J. C. Collison (2002), Quantifying the mechanical and hydrologic effects of riparian vegetation on streambank stability, *Earth Surf. Processes Landforms*, 27, 527-546.
- Smith, C. E. (1998), Modeling high sinuosity meanders in a small flume, *Geomorphology*, 25, 19-30.
- Smith, S. M., and K. L. Prestegard (2005), Hydraulic performance of a morphology-based stream channel design, *Water Resour. Res.*, 41, doi:10.1029/2004WR003926.
- Stillwater Sciences (2001), Merced River restoration baseline studies, Volume II, geomorphic and riparian vegetation investigations report, final report, 226 pp., Berkeley, Calif.
- Tal, M., K. Gran, A. B. Murray, C. Paola, D. and M. Hicks (2004), Riparian vegetation as a primary control on channel characteristics in multi-thread rivers, in *Riparian Vegetation and Fluvial Geomorphology: Hydraulic, Hydrologic, and Geotechnical Interaction*, edited by S. J. Bennett and A. Simon, pp. 43-58, AGU, Washington, D.C.
- Tal, M., and C. Paola (2007), Dynamic single-thread channels maintained by the interaction of flow and vegetation, *Geology*, 35, 347-350.
- Thorne, C. R. (1982), Processes and mechanisms of river bank erosion, in *Gravel-bed rivers*, edited by Hey, R. D., J.C. Bathurst, and C. R. Thorne, pp. 227-271, John Wiley & Sons Ltd., Chichester, U.K.
- Thorne, C. R. (1990), Effects of vegetation on riverbank erosion and stability, in *Vegetation and Erosion*, edited by J. B. Thornes, pp. 125-144, John Wiley and Sons, Chichester, U.K.
- Whiting, P. J. and W. E. Dietrich (1993), Experimental constraints on bar migration through bends: implications for meander wavelength selection, *Water Resour. Res.*, 29, 1091-1102.

- Williams, G. P., and M. G. Wolman (1984), Downstream effects of dams on alluvial rivers, *Geological Survey Professional Paper 1286*, 88 pp., U.S. Geol. Surv., Washington, D. C.
- Williams, J. E., C. A. Wood, and M. P. Dombeck (1997), Understanding watershed-scale restoration, in *Watershed Restoration: Principles and Practices*, edited by J. E. Williams, C. A. Wood, and M. P. Dombeck, pp. 1-16, Am. Fish. Soc., Bethesda, Md.
- Wohl, E., P. L. Andermeier, B. Bledsoe, G. M. Kondolf, L. MacDonnell, D. M. Merritt, M. A. Palmer, N. L. Poff, and D. Tarboton (2005), River restoration, *Water Resour. Res.*, *41*, W10301, doi:10.1029/2005WR003985.
- Wolman, M. G. and J. P. Miller (1960), Magnitude and frequency of forces in geomorphic processes, *J. of Geol.*, *68*, 54-74.
- Wong, M. and G. Parker (2006a), One-dimensional modeling of bed evolution in a gravel bed river subject to a cycled hydrograph, *J. Geophys. Res.*, *111*, F03018, doi:10.1029/2006JF000478.
- Wong, M. and G. Parker (2006b), Reanalysis and correction of bed-load relation of Meyer-Peter and Müller using their own database, *J. Hydraul. Eng.*, doi:10.1061/(ASCE)0733-9429(2006)132:11(1159).
- Yen, C. and K. T. Lee (1995), Bed topography and sediment sorting in channel bend with unsteady flow, *J. Hydraul. Eng.*, *8*, 591-599.

**LIST OF TABLES**

**Table 1. Initial model channel parameters.**

Parameter	Notation	Value
Median grain size of floodplain and channel	$D_{fp50}$	1 mm
Median grain size of bedload feed	$D_{bf50}$	0.8 mm
Median grain size of fine silica applied to floodplain surface	$D_{sil50}$	0.027 mm
Floodplain slope	$S_{fp}$	0.005
Channel width	$W$	50 cm
Channel depth	$H$	1.7 cm
Channel aspect ratio	$W:H$	30

**Table 2. Input parameters and measured data.**

Run	Run Step	$t$ , hr	$Q_w$ , L/s	$S_{ws}$	$u$ , cm/s	$w_{XS1.5m}$ , cm	$Q_{s-in}$ , kg/hr	$Q_{s-out}$ , kg/hr	$\Delta S$ , kg	$D_{out1\sigma}$ , (mm)	$D_{out50}$ , (mm)	$D_{out8\sigma}$ , (mm)
6.1	1	1.75	0.2-1.3	0.0042	24.0	5.52	0	0	0			
	2	0.75	1.6	0.0041	28.0	5.52	3.8	0	2.9			
	3	5	1.9	0.0044	31.2	5.52	3.8	1.6	11.1	0.4	0.8	1.5
6.2	1	0.5	1.0	0.0039	25.6	5.52	0.4	0.2	0.1	0.3	0.6	1.4
	2	0.5	2.2	0.0046	32.8	5.52	3.8	4.7	-0.4	0.3	0.8	1.5
	3	0.52	3.3	0.0046	35.2	5.70	12.6	9.9	1.4	0.3	0.8	1.4
	4	0.52	4.4	0.0046	40.0	5.98	18.8	13.9	2.6	0.3	0.8	1.4
	5	0.5	3.3	0.0047	35.2	5.98	12.6	12.6	0	0.4	0.7	1.4
	6	1.53	2.2	0.0048	34.0	6.24	3.8	7.7	-6.0	0.3	0.6	1.3
	7	2.5	1.0	0.0040	27.2	6.24	0.4	0.4	-0.1	0.3	0.8	1.4
6.3	1	0.52	1.0	0.0040	29.6	6.54	0.4	1.5	-0.6	0.4	0.9	1.5
	2	0.5	2.2	0.0044	33.6	6.88	4.4	5.2	-0.4	0.3	0.7	1.4
	3	0.5	3.3	0.0046	36.8	7.23	12.6	9.8	1.4	0.3	0.8	1.5
	4	0.5	4.4	0.0047	38.4	7.52	18.8	12.3	3.2	0.3	0.8	1.5
	5	0.5	3.3	0.0050	34.4	7.52	12.6	9.3	1.6	0.3	0.6	1.4
	6	1.4	2.2	0.0049	32.8	7.64	3.8	6.4	-3.6	0.3	0.6	1.3
	7	2.5	1.0	0.0046	26.8	7.64	0.4	0.4	-0.1	0.3	0.6	1.3

<sup>a</sup>Notation includes  $t$ , run step duration;  $Q_w$ , discharge;  $S_{ws}$ , water surface slope;  $u$ , mean depth-average flow velocity,  $w_{XS1.5m}$ , channel width taken at cross-section XS 1.5m,  $Q_{s-in}$ , sediment feed rate;  $Q_{s-out}$ , sediment transport rate out (determined from mass collected per step divided by the duration);  $\Delta S$ , change in sediment storage (i.e., mass balance);  $D_{out1\sigma}$ , transported material grain size at one standard deviation less than the median;  $D_{out50}$ , median transported material grain size;  $D_{out8\sigma}$ , transported material grain size at one standard deviation greater than the median.

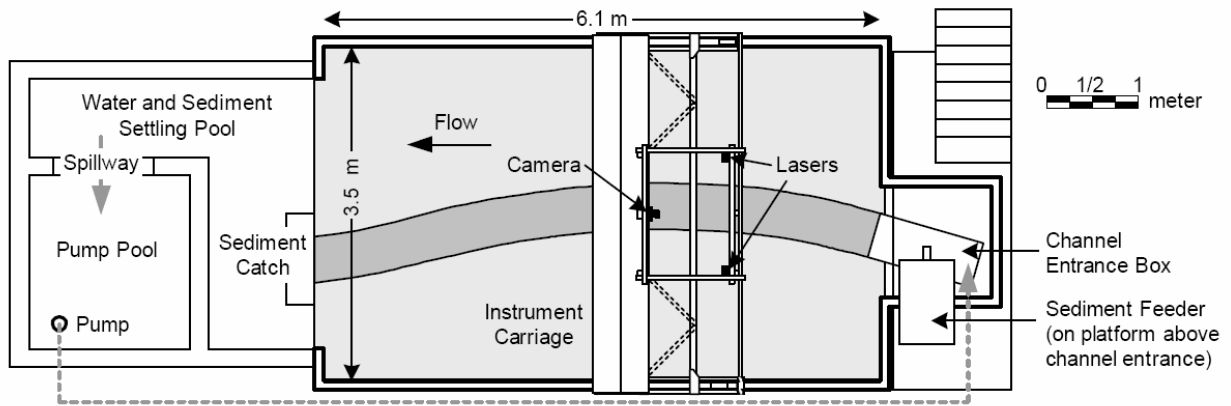


**Figure 1.** Schematic of the small flume basin at UC Berkeley Richmond Field Station hydraulics laboratory.

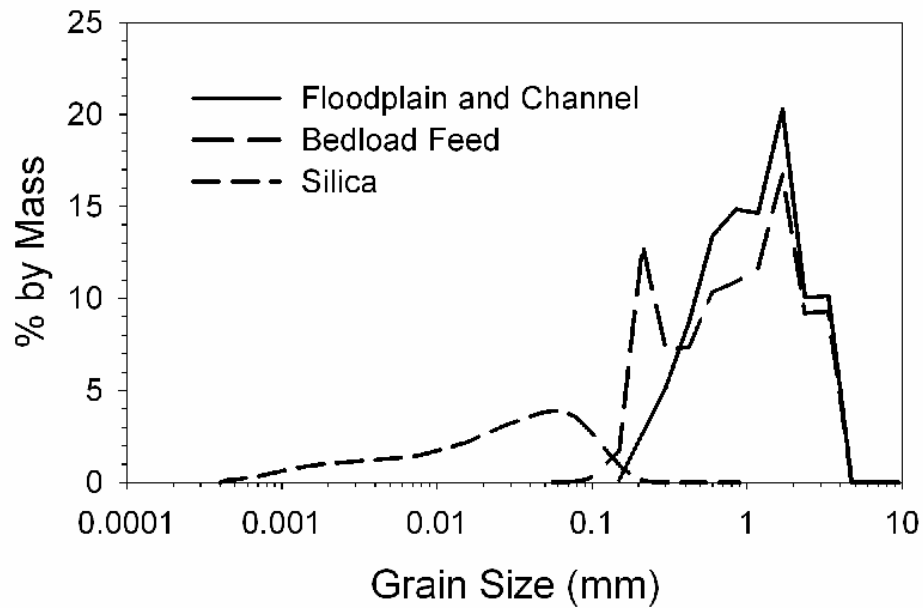


**Figure 2.** Percent by mass particle size distribution of floodplain and channel sediment mixture, bedload feed sediments, and silica applied to the floodplain surface.



**Figure 3.** Alfalfa sprouts used to provide bank strength. Sand particles (model gravel) are cohesively attached to sprout roots.

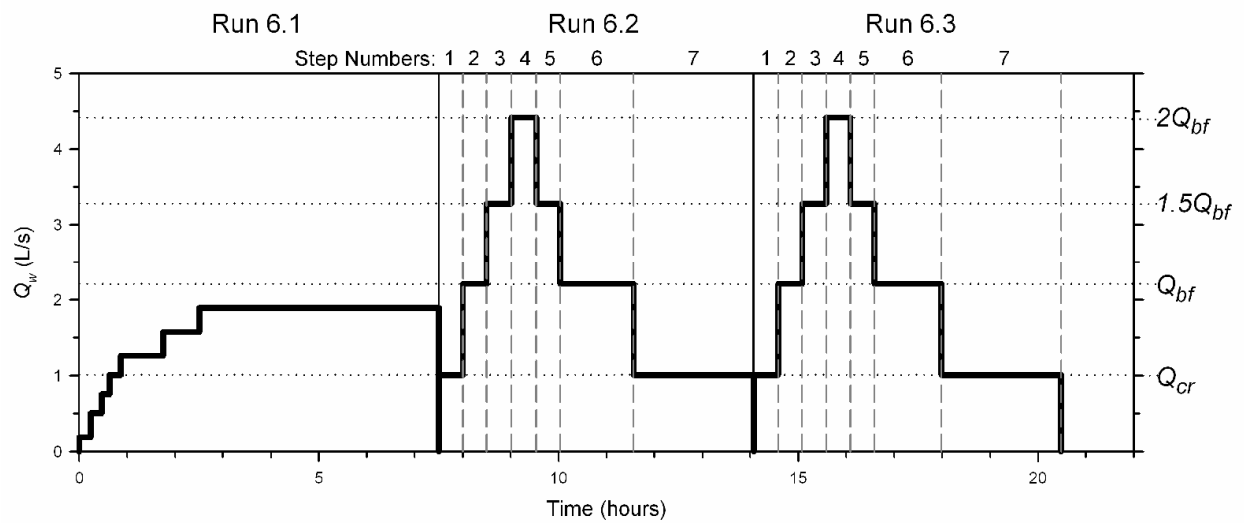


**Figure 4.** Hydrographs of the experiments, that include: Run 6.1 (Initial Condition), Run 6.2 (Hydrograph #1), and Run 6.3 (Hydrograph #2).

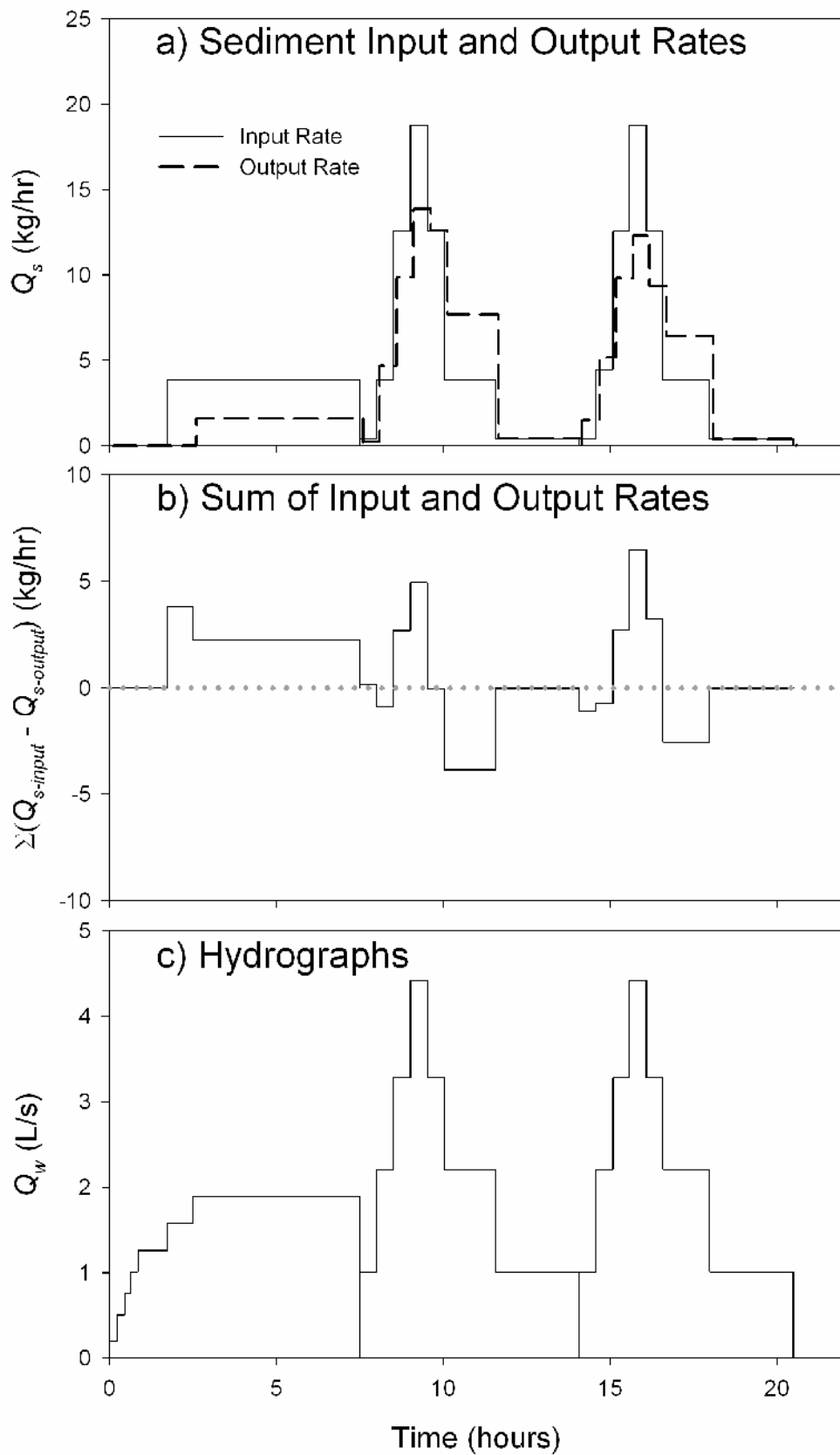


**Figure 5.** Sediment input and output rates (z) and their difference (b) at each step of the experimental runs shown relative to the hydrographs (c).

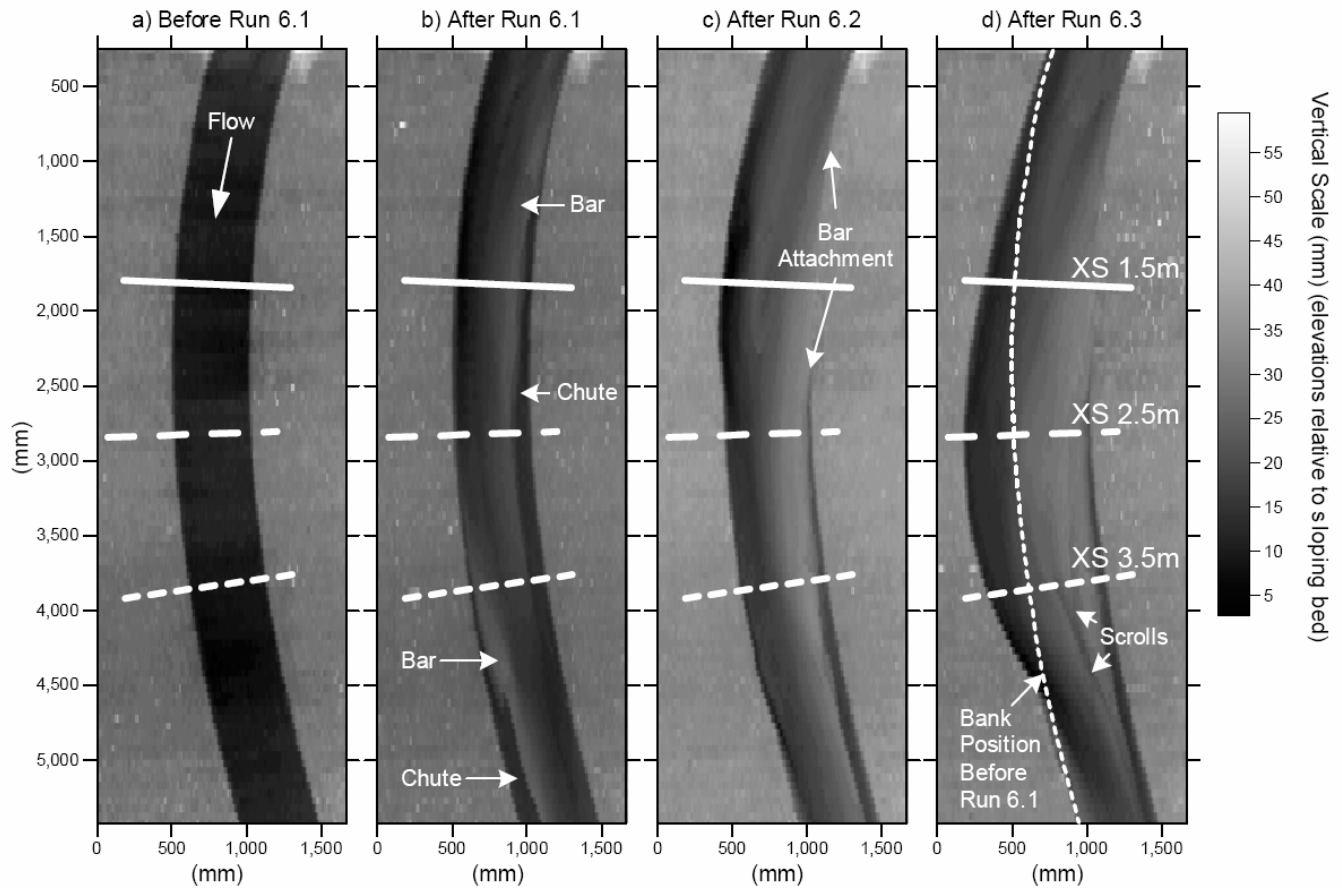


**Figure 6.** Planform evolution of channel showing morphology before (a) and after (b) Run 6.1, after (c) Run 6.2, and after (d) Run 6.3. Flow moved through the channel from the top to bottom. Three cross-sections are referenced: XS 1.5m, XS 2.5m, and XS 3.5m. Bar-pool development (b) initiated during Run 6.1 (Initial Condition Run). Point bar attachment through chute filling occurred during Run 6.2 (Hydrograph #1). The point bar front and outer bank positions advanced laterally (c and d) during Runs 6.2 and 6.3 (Hydrographs #1 and #2). Scroll features developed along the downstream end of the bar during the overbank flow steps of Run 6.3.

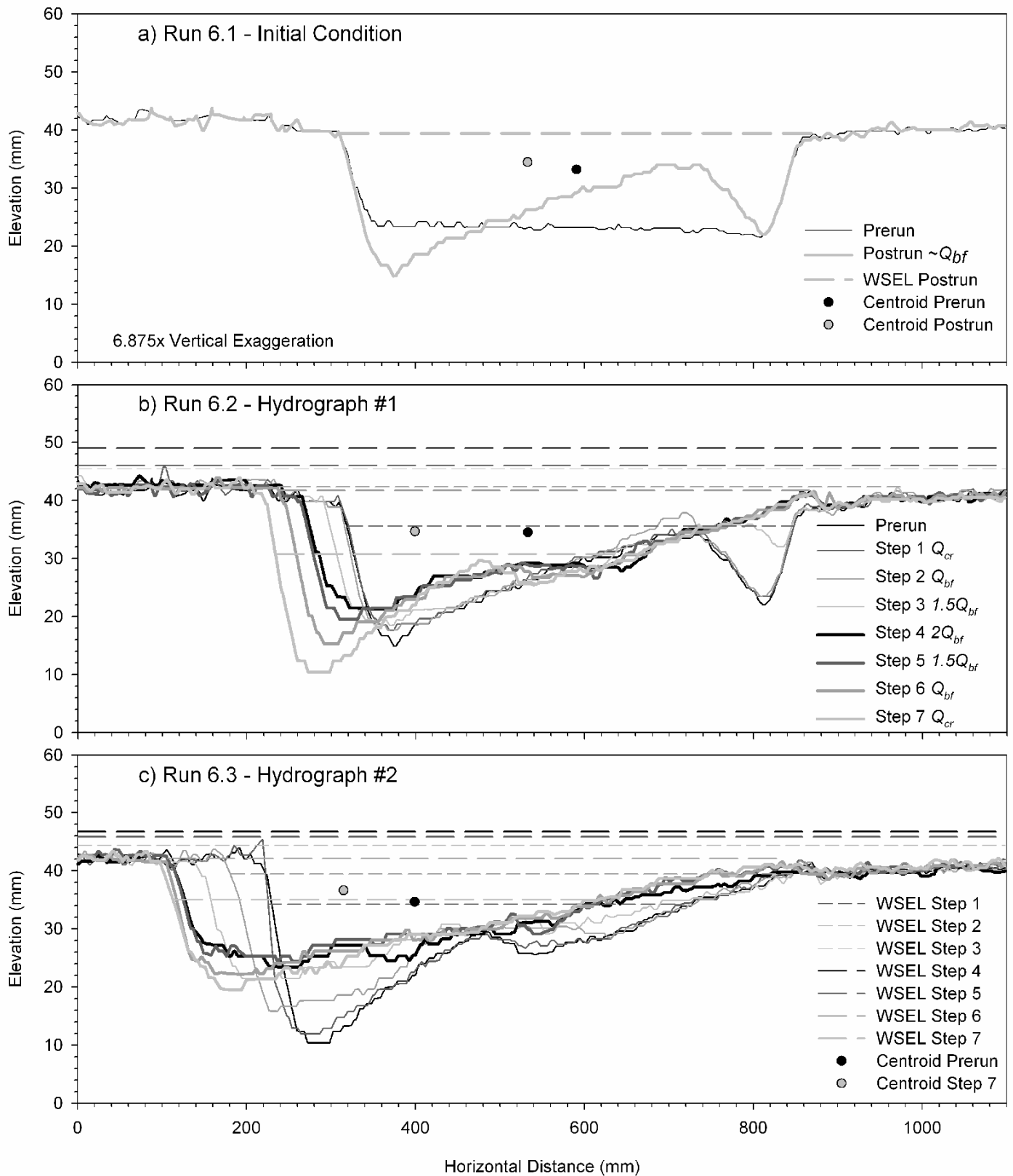


**Figure 7.** Cross-section (XS) evolution in response to flow and sediment feed variations at XS 1.5 m looking upstream. Bar-pool development (a) initiated with bankfull discharge during Run 6.1 (Initial Condition). The point bar connected to the inner bank (b) as the bar grew vertically and sediment filled in the chute during Steps 3 ( $1.5Q_{bf}$ ) and 4 ( $2Q_{bf}$ ) of Run 6.2 (Hydrograph #1). Lateral migration continued (c) with near-equal rates of bar growth and bank erosion during Run 6.3 (Hydrograph #2). Water surface elevations (WSEL) per step are shown relative to the resulting cross-section. For each run, the geometric centroids of the initial and final channel forms are shown which indicate: 1) lateral migration through bank retreat and bar advancement, and 2) relatively small net changes in the bed elevation.



**Figure 8.** View looking downstream after Run 6.3. Coarser sediments transported and deposited along the channel thalweg (center of image) while finer sediments were selectively transported to and deposited on the bar (left side of image).

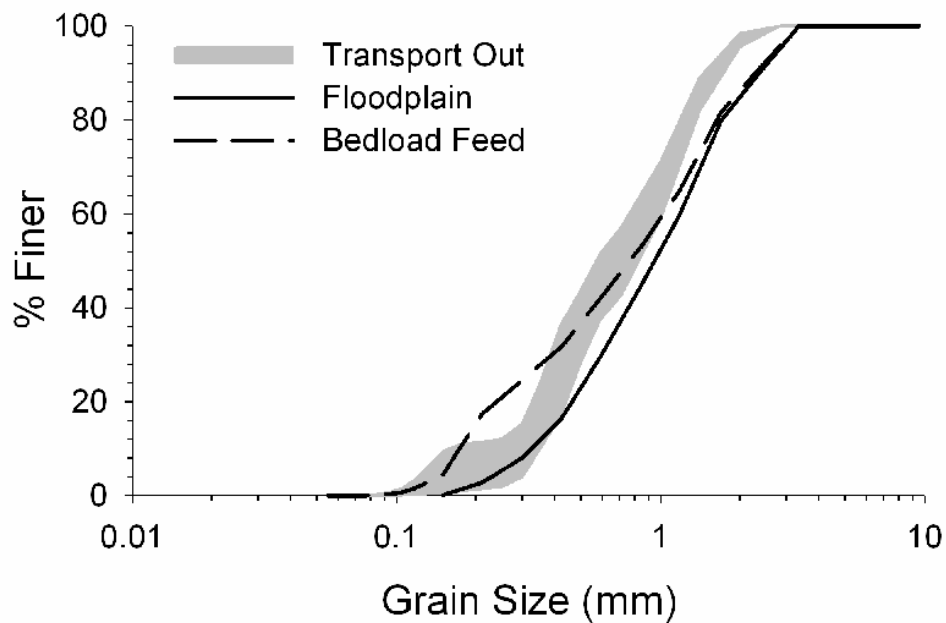


**Figure 9.** Grain size distribution range of transported sediment from all 15 run steps with floodplain and bedload feed size distributions shown for reference. The range between the maxima and minima of percent finer values for a given grain size are represented by the vertical thickness of the plotted data.

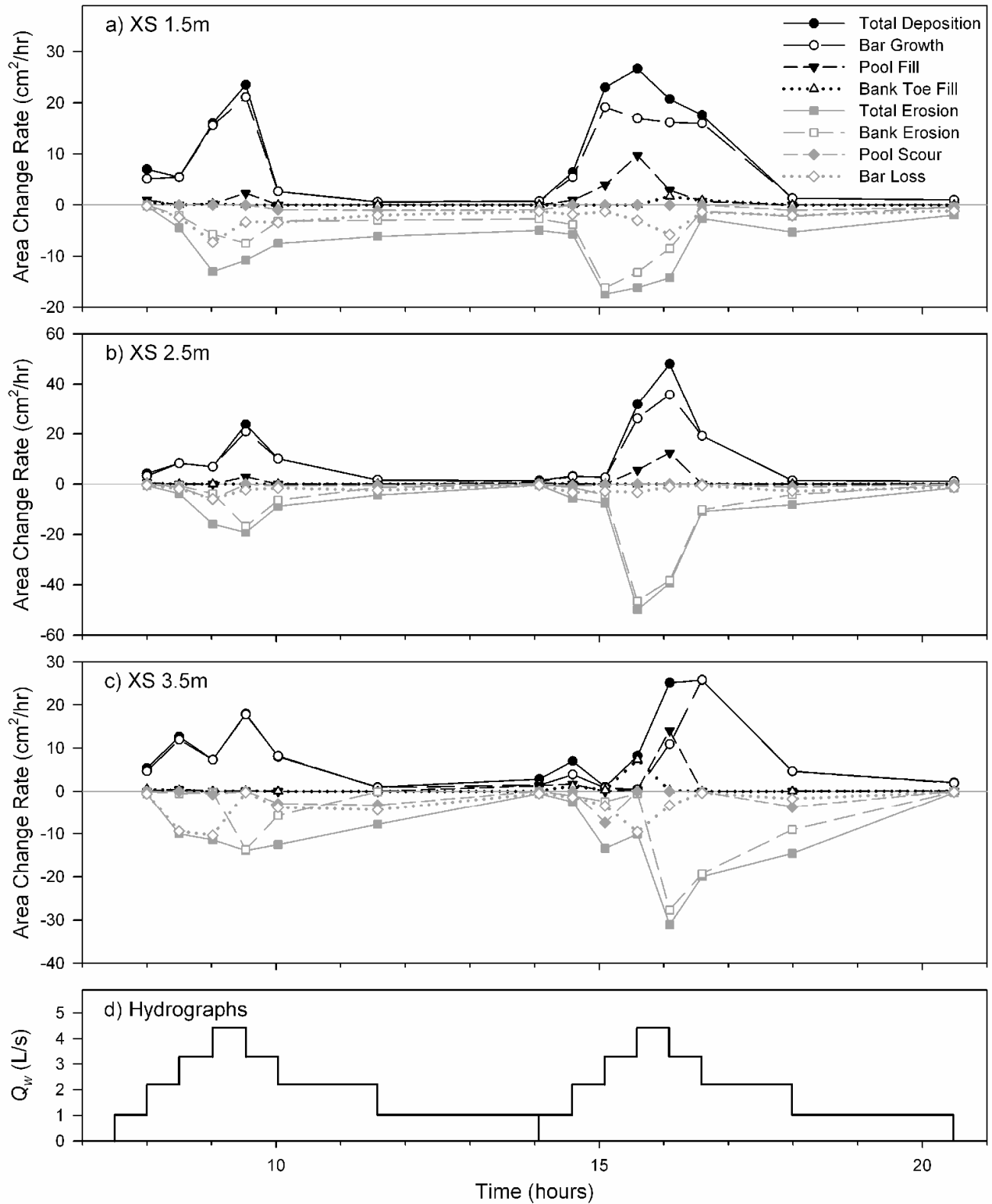


**Figure 10.** The rates of channel component area change at three locations along the channel bend (XS 1.5m, XS 2.5m, and XS 3.5m) shown relative to the two hydrograph runs. The total deposition and total erosion rates per step are shown, as are their respective components including bar growth, pool fill, and bank toe fill, and bank erosion, pool scour, and bar loss (see Figure 11 for explanation of components).

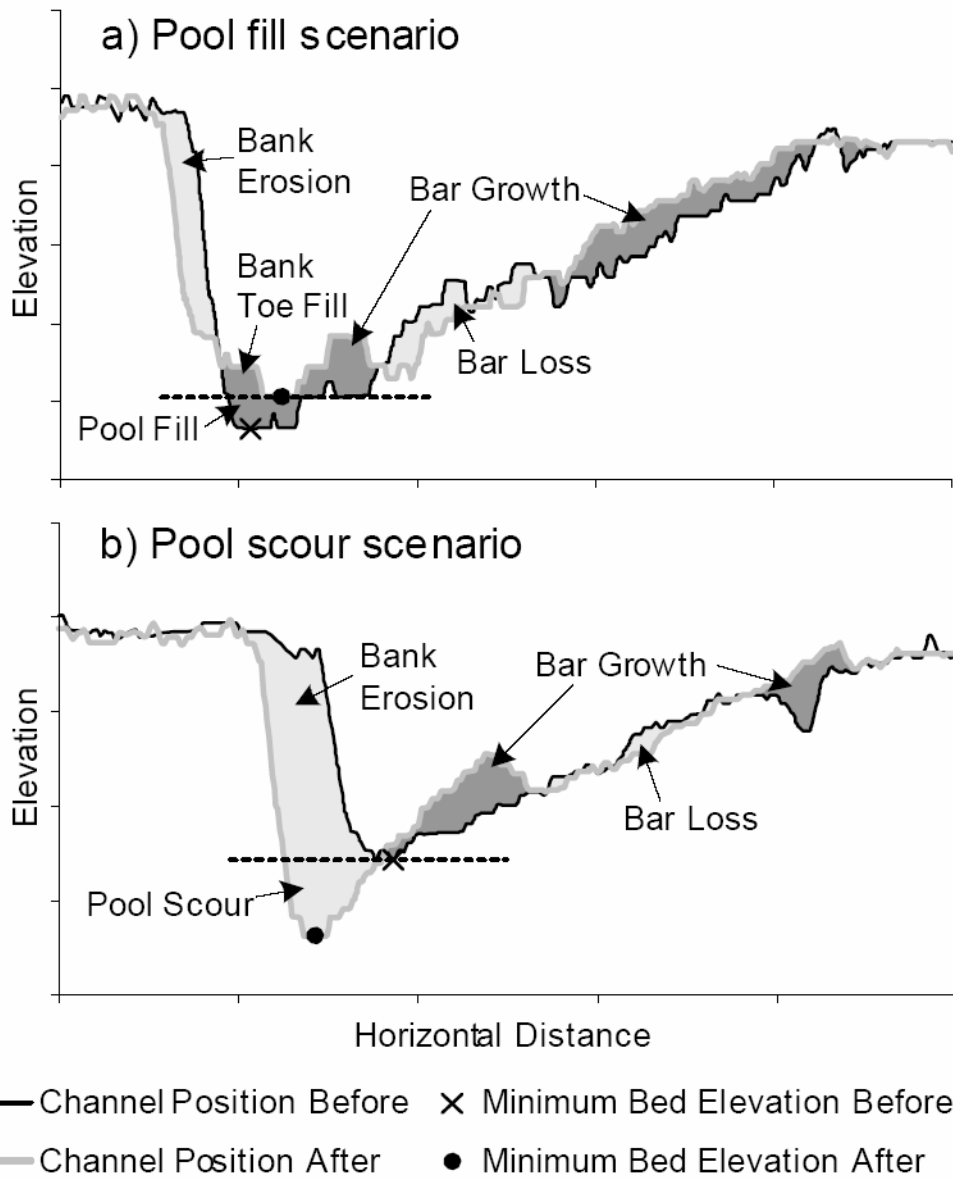


**Figure 11.** Definitions of channel area components in cross-section. The two examples illustrate how the total positive (i.e., deposition) and total negative (i.e., erosion) areas bounded between successive cross-sections were each divided to define the channel area components. A rise in the minimum bed elevation (a) leads to pool fill. Deposition upon the bar side of the minimum bed elevation is defined as bar growth. Erosion on that side is bar loss. Erosion on the bank side of the minimum bed elevation is defined as bank erosion. Any deposition adjacent to the bank on that side is defined as bank toe fill. Lowering of the minimum bed elevation (b) leads to pool scour.

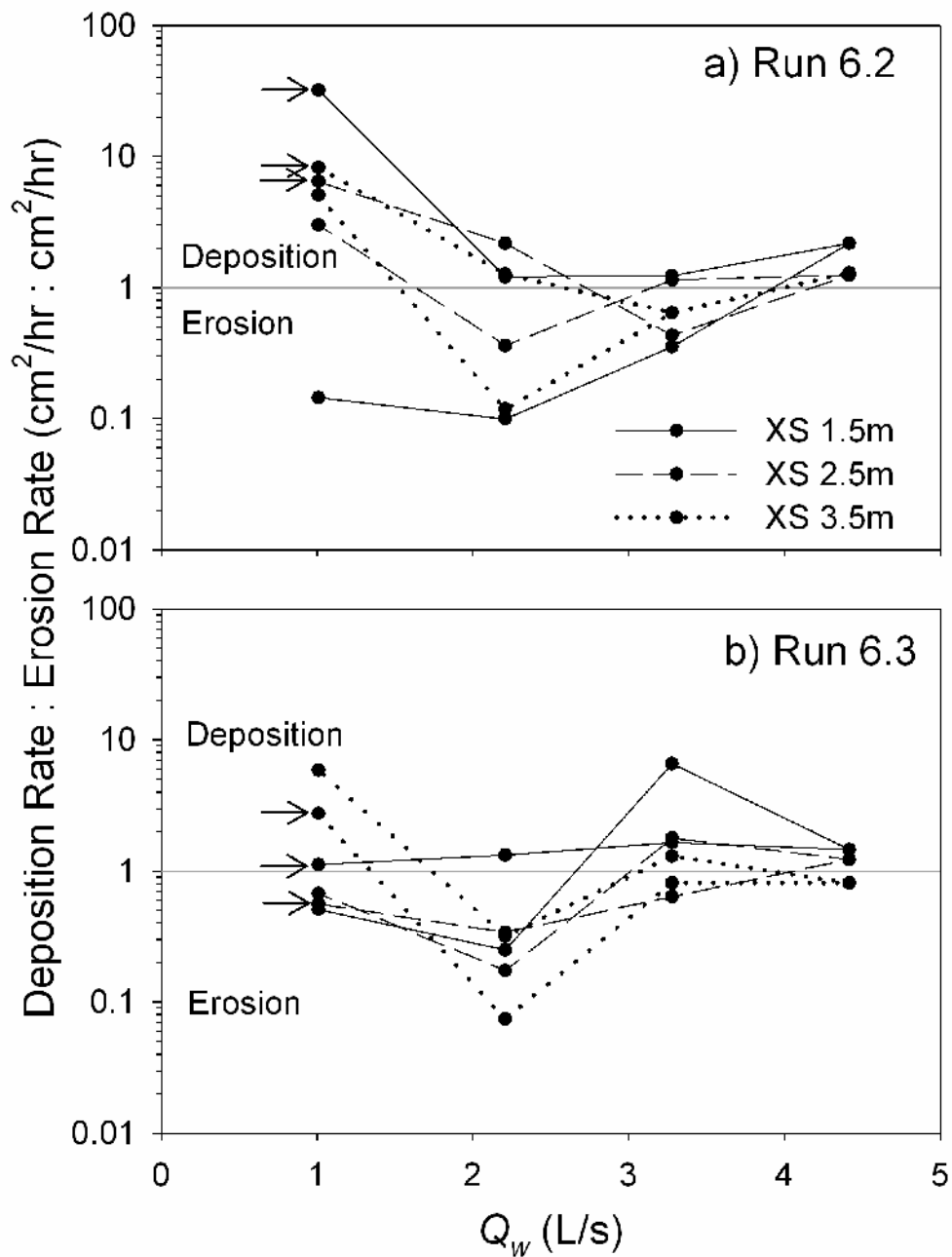


**Figure 12.** Relationship between total deposition rates and total erosion rates as a function of discharge during the two hydrograph runs (Runs 6.2 and 6.3) at three cross-sections along the channel bend: XS 1.5m, XS 2.5m, and XS 3.5m. Plotted values greater than one indicate greater deposition rates than erosion rates, and values less than one indicate greater erosion rates than deposition rates. The direction of hysteresis within each cross-section's dataset is indicated by an arrow pointing to the initial data point.

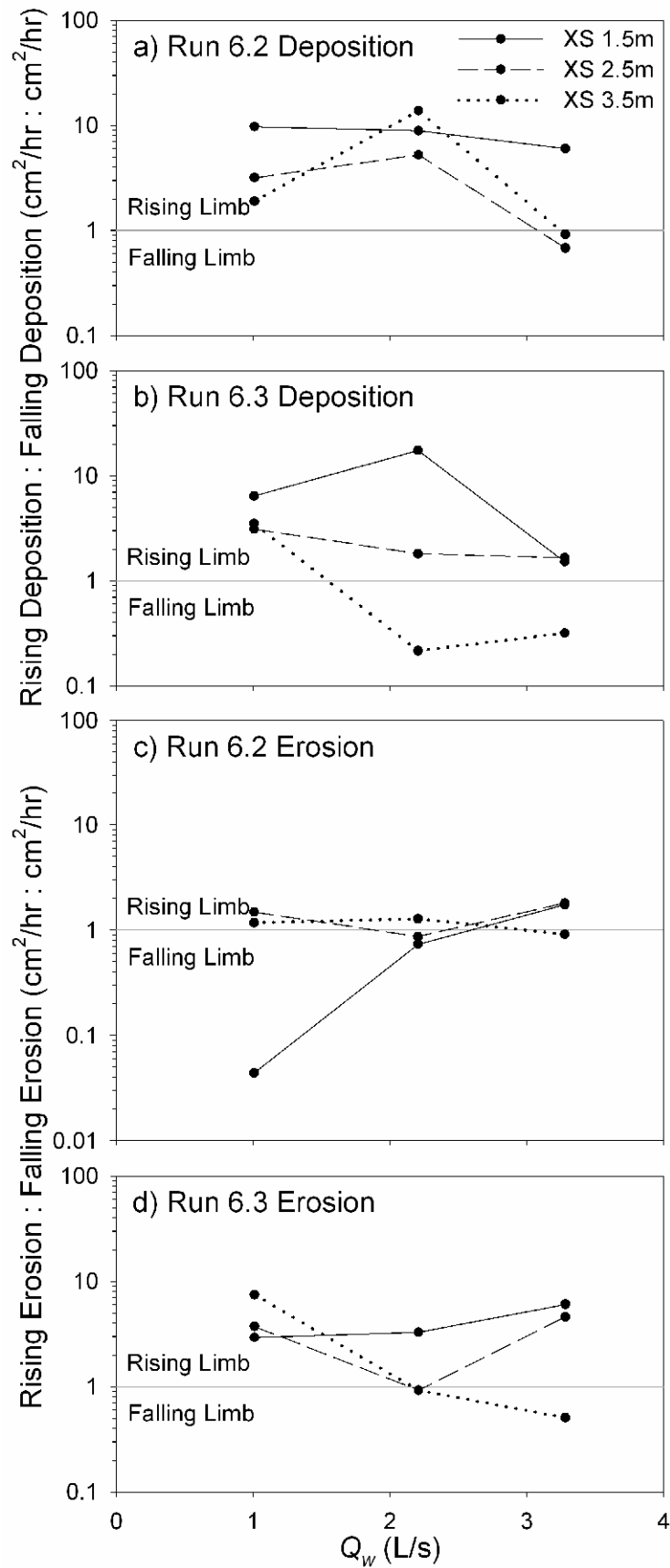


**Figure 13.** Comparisons of channel change in cross-section during the rising and falling limbs of the two hydrograph runs (Runs 6.2 and 6.3) at three cross-sections along the channel bend: XS 1.5m, XS 2.5m, and XS 3.5m. Total deposition rates during the rising and falling limbs are compared (a, b) at common discharges, as are the total erosion rates (c, d). Plotted values greater than one indicate greater rates of change during the falling limb.